NETWORKS AND HETEROGENEOUS MEDIA
©American Institute of Mathematical Sciences
Volume **8**, Number **2**, June **2013**
doi:10.3934/nhm.2013.8.433
pp. **433–463**

GENERAL CONSTRAINED CONSERVATION LAWS. APPLICATION TO PEDESTRIAN FLOW MODELING

Christophe Chalons

Univ. Paris Diderot, Sorbonne Paris Cité
Laboratoire Jacques-Louis Lions, UMR 7598, UPMC, CNRS
F-75205 Paris, France

Paola Goatin and Nicolas Seguin

INRIA Sophia Antipolis - Méditerranée, EPI OPALE
2004, route des Lucioles - BP 93
F-06902 Sophia Antipolis Cedex, France

UPMC Univ Paris 06, Laboratoire Jacques-Louis Lions, UMR 7598, CNRS
F-75005, Paris, France
& INRIA Paris-Rocquencourt, Equipe ANGE - BP 105
F-78153 le Chesnay Cedex, France

(Communicated by Benedetto Piccoli)

Abstract. We extend the results on conservation laws with local flux constraint obtained in [2, 12] to general (non-concave) flux functions and non-classical solutions arising in pedestrian flow modeling [15]. We first provide a well-posedness result based on wave-front tracking approximations and the Kružhkov doubling of variable technique for a general conservation law with constrained flux. This provides a sound basis for dealing with non-classical solutions accounting for panic states in the pedestrian flow model introduced by Colombo and Rosini [15]. In particular, flux constraints are used here to model the presence of doors and obstacles. We propose a "front-tracking" finite volume scheme allowing to sharply capture classical and non-classical discontinuities. Numerical simulations illustrating the Braess paradox are presented as validation of the method.

1. **Introduction.** Several phenomena displayed by vehicular traffic can be modeled using conservation laws in one space-dimension, see for example [22] for a survey of available models. In particular, specific situations as the presence of toll gates, construction sites, or even moving bottlenecks caused by slow moving large vehicles, can be realistically modeled by imposing a local constraint on the flux, see [12, 13, 14, 19, 21]. In all these works, the flux function of the involved model is assumed to be concave, which strongly simplifies the structure and the analysis of solutions.

Besides, Colombo and Rosini [15] introduced a model for pedestrian flow accounting for panic appearance and consisting in a scalar conservation law in one space-dimension displaying nonclassical shocks. Such a simplified model can be used

2010 *Mathematics Subject Classification.* Primary: 35L65; Secondary: 90B20.

Key words and phrases. Constrained scalar conservation laws, finite volume schemes, non-classical shocks, macroscopic pedestrian flow models, Braess paradox.

The second author was partially supported by the ERC Starting Grant 2010 under the project *"TRAffic Management by Macroscopic Models"*.

for example to describe the motion of a crowd along a corridor or a bridge. Moreover, in [16] the authors show that the flux constraint represented by the presence of a door may cause the onset of panic states from a normal situation. In this model, the flux function is not concave (nor convex) and therefore it does not match the available results about conservation laws with constrained flux. A rigorous analysis of this pedestrian flow model thus needs the extension of the above cited results to general fluxes. Moreover, the study of the non-convex case constitutes a non-trivial generalization which is interesting from the analytical point of view.

In this paper, we are interested in the Cauchy problem for scalar conservation laws with local unilateral constraint of the form

$$\partial_t \rho + \partial_x f(\rho) = 0, \qquad t > 0,\ x \in \mathbb{R}, \tag{1}$$

$$\rho(0,x) = \rho_0(x), \qquad x \in \mathbb{R}, \tag{2}$$

$$f(\rho(t,0)) \leq F(t), \qquad t > 0. \tag{3}$$

Having in mind the pedestrian flow model described in [15], we fix $R > 0$ to be the maximal density supported by the model and we assume that the flux function $f : [0,R] \to \mathbb{R}$ is Lipschitz continuous with Lipschitz constant L

(F.1) $f \in \mathbf{W}^{1,\infty}([0,R];[0,+\infty[)$ and piecewise $\mathbf{C^1}$

(so that left and right derivatives $f'(\rho\pm)$ are well defined for all $\rho \in [0,R]$), and satisfies

(F.2) $f(\rho) \geq 0, \quad f(0) = f(R) = 0,$

(F.3) there exists a finite set of points $\{\rho_1, \dots, \rho_N\} \subset [0,R]$, $N \geq 1$, which are strict local minima or maxima of f, i.e. $f(\rho) - f(\rho_i) < 0$ (or > 0) for ρ in a neighborhood of ρ_i, $i = 1, \dots, N$, and $f'(\rho\pm) \neq 0$ for all $\rho \in [0,R] \setminus \{\rho_1, \dots, \rho_N\}$.

We will also denote by $f_{\max}$ the maximum of f on $[0,R]$:

$$f_{\max} = \max_{\rho \in [0,R]} f(\rho).$$

The paper is organized as follows. In Section 2 we define the constrained Riemann solver and the entropy condition associated to (1)-(3). This allows to prove a well posedness result based on wave-front tracking approximations and Kruzhkov doubling of variable technique. (Details of the proof are collected in Section 5.) Section 3 revises the finite volume scheme introduced in [2]. Finally, Section 4 deals with the pedestrian flow model proposed in [15]: we define the constrained non-classical Riemann solver and we propose a "front-tracking" finite volume scheme allowing to sharply capture classical and non-classical discontinuities, and to verify the flux constraint. Numerical simulations illustrating the Braess paradox are presented in Section 4.5.

2. Well posedness.

2.1. Definition of the constrained Riemann solver.

Let $\mathcal{R}$ be the standard Riemann solver for (1), (2), with

$$\rho(0,x) = \begin{cases} \rho_l \text{ if } x < 0, \\ \rho_r \text{ if } x > 0, \end{cases} \tag{4}$$

whose first descriptions in the scalar case date back to Gel'fand [23] and Dafermos [18]. More precisely, the map $(t,x) \mapsto \mathcal{R}(\rho_l,\rho_r)(x/t)$ is the standard weak entropy solution to (1),(4).

Let $F(t) \equiv F \in [0, f_{\max}]$ be constant, and $\rho_1^F, \dots, \rho_M^F \in [0,R]$, $1 \le M \le N+1$, be the roots of the equation

$$f(\rho) = F.$$

In connection with (4), we denote

$$\hat\rho_l^F = \begin{cases} \min\left\{\rho_1^F,\dots,\rho_M^F : \rho_i^F \ge \rho_l\right\} & \text{if } f(\rho_l) > F \\ \max\left\{\rho_1^F,\dots,\rho_M^F : \rho_i^F \le \rho_l\right\} & \text{if } f(\rho_l) \le F \end{cases} \tag{5}$$

$$\check\rho_r^F = \begin{cases} \max\left\{\rho_1^F,\dots,\rho_M^F : \rho_i^F \le \rho_r\right\} & \text{if } f(\rho_r) > F \\ \min\left\{\rho_1^F,\dots,\rho_M^F : \rho_i^F \ge \rho_r\right\} & \text{if } f(\rho_r) \le F \end{cases} \tag{6}$$

whenever $\rho_l > \rho_1^F$, respectively $\rho_r < \rho_M^F$. We note here that, as showed below, if $\rho_l \le \rho_1^F$ and $\rho_r \ge \rho_M^F$ the solution of the constrained Riemann problem coincides with the non-constrained one, and (5), (6) are of no use in the following definition.

Definition 2.1. The constrained Riemann solver $\mathcal{R}^F : (\rho_l,\rho_r) \mapsto \mathcal{R}^F(\rho_l,\rho_r)$ for (1)-(3) is defined as follows.
If $f\left(\mathcal{R}(\rho_l,\rho_r)(0)\right) \le F$, then $\mathcal{R}^F(\rho_l,\rho_r) = \mathcal{R}(\rho_l,\rho_r)$.
Otherwise, $\mathcal{R}^F(\rho_l,\rho_r)(\lambda) = \begin{cases} \mathcal{R}(\rho_l,\hat\rho_l^F)(\lambda) \text{ if } \lambda < 0\,, \\ \mathcal{R}(\check\rho_r^F,\rho^r)(\lambda) \text{ if } \lambda > 0\,. \end{cases}$

We now check that Definition 2.1 defines a self-similar weak solution to (1), (4), subject to the constant constraint F. First of all, we note that the stationary discontinuity between $\hat\rho_l^F$ and $\check\rho_r^F$ at $x=0$ satisfies Rankine-Hugoniot condition, since $f(\hat\rho_l^F) = F = f(\check\rho_r^F)$ by (5), (6).

Next, let us remind that the classical entropy Riemann solver satisfies

$$f\left(\mathcal{R}(\rho_l,\rho_r))(0)\right) = \begin{cases} \min\limits_{\rho\in[\rho_l,\rho_r]} f(\rho) & \text{if } \rho_l \le \rho_r\,, \\ \max\limits_{\rho\in[\rho_r,\rho_l]} f(\rho) & \text{if } \rho_r < \rho_l\,. \end{cases} \tag{7}$$

Let us analyze the left-hand side of the solution (i.e. for $\lambda < 0$, the analysis for $\lambda > 0$ being similar). First of all, let us observe that if $f\left(\mathcal{R}(\rho_l,\rho_r)(0)\right) > F$, then (7) implies $\rho_l > \rho_1^F$. We have to distinguish several cases.

- If $\rho_l \le \rho_1^F$, we have by (7)
$$f\left(\mathcal{R}(\rho_l,\rho_r)(0)\right) \le F, \text{ hence } \mathcal{R}^F(\rho_l,\rho_r) = \mathcal{R}(\rho_l,\rho_r).$$
- If $f(\rho_l) > F$, then by (5) $\hat\rho_l^F > \rho_l$ and (7) implies
$$f\big(\mathcal{R}(\rho_l,\hat\rho_l^F)(0)\big) = \min_{\rho\in[\rho_l,\hat\rho_l^F]} f(\rho) = f(\hat\rho_l^F) = F,$$
hence $\mathcal{R}(\rho_l,\hat\rho_l^F)$ does not contain waves with positive speed.
- If $f(\rho_l) \le F$ and $\rho_l > \rho_1^F$, then by (5) $\hat\rho_l^F \le \rho_l$ and (7) implies
$$f\big(\mathcal{R}(\rho_l,\hat\rho_l^F)(0)\big) = \max_{\rho\in[\hat\rho_l^F,\rho_l]} f(\rho) = f(\hat\rho_l^F) = F,$$
hence again $\mathcal{R}(\rho_l,\hat\rho_l^F)$ does not contain waves with positive speed.

Remark 1. The stationary jump from $\hat\rho_l^F$ to $\check\rho_r^F$ doesn't satisfy the Liu's entropy condition [28]. In fact, two cases can occur if $f\left(\mathcal{R}(\rho_l,\rho_r))(0)\right) > F$:

- If $\rho_l < \rho_r$, then by (7) we infer that $f(\rho_l), f(\rho_r) > F$ and therefore $\check\rho_r^F \le \rho_l < \rho_r \le \hat\rho_l^F$ by (5), (6).

- If $\rho_l > \rho_r$, then (7) implies that there exists $\rho^* \in [\rho_r, \rho_l]$ such that $f(\rho^*) > F$. Therefore, by (5), (6) we can conclude that $\check{\rho}_r^F \leq \rho^* \leq \hat{\rho}_l^F$.

In both cases, Liu's entropy condition is not satisfied. We will refer to such discontinuities as *non-classical shocks*.

2.2. **Entropy conditions.** Having in mind the analysis of the model for pedestrian flow introduced in [15], and in order to reduce technicalities and the number of cases to be considered, from now on we will restrict the study to flux functions that fit the hypotheses in [16]. Nevertheless, we believe that the results hold true for more general fluxes. We will require the following properties (see Fig. 2, right, in Section 4.1):

(F.2) $f(\rho) = 0$ if and only if $\rho \in \{0, R\}$;
(F.3.1) f has a local minimum at $r \in [0, R]$
(F.3.2) the restrictions $f_{|[0,r]}$ and $f_{|[r,R]}$ are strictly concave;
(F.3.3) $f(r_M) = \max\{f(\rho)\colon \rho \in]0, r[\} > f(R_M) = \max\{f(\rho)\colon \rho \in]r, R[\}$.

Further requirements will be added in Section 4.1.

The definitions of entropy weak solutions introduced in [2, 12] can be generalized to the present case. Let us introduce the function

$$\Phi(a, b) = \operatorname{sgn}(a - b)\,(f(a) - f(b)) = f(a \top b) - f(a \perp b),$$

where $a \top b = \max\{a, b\}$ and $a \perp b = \min\{a, b\}$.

Definition 2.2. A function $\rho \in \mathbf{L}^\infty(\mathbb{R}^+ \times \mathbb{R}; [0, R])$ is a weak entropy solution of (1)-(3) if
(i) it satisfies the following entropy inequalities: for every $\varphi \in \mathbf{C_c^1}(\mathbb{R}^+ \times \mathbb{R}; \mathbb{R}^+)$ and all $\kappa \in [0, R]$,

$$\int_0^{+\infty} \int_{\mathbb{R}} \left(|\rho(t,x) - \kappa|\partial_t + \Phi(\rho(t,x), \kappa)\partial_x\right) \varphi(t,x)\, dx\, dt + \int_{\mathbb{R}} |\rho_0(x) - \kappa|\, \varphi(0,x)\, dx + 2\int_0^{+\infty} \left(f(\kappa) - f(\kappa) \perp F(t)\right) \varphi(t,0)\, dt \geq 0, \quad (8)$$

(ii) it verifies the constraint:

$$f(\rho(t,0-)) = f(\rho(t,0+)) \leq F(t) \quad \text{for a.e. } t > 0, \quad (9)$$

where $\rho(t, 0\pm)$ denote the operators of left and right strong traces at $\{x = 0\}$.

It is easy to check that the constrained Riemann solver introduced in Definition 2.1 gives a weak entropy solution of (1)-(3) in the sense of the above Definition 2.2.

Proposition 1. *Let $\rho(t,x) = \mathcal{R}^F(\rho_l, \rho_r)(x/t)$ be the weak solution to (1), (3) and (4) constructed in Definition 2.1. Then ρ is a weak entropy solution in the sense of Definition 2.2. Moreover, the entropy condition (8) and the constraint (9) single out the maximal stationary discontinuities satisfying the constraint.*

Proof. Let us consider an admissible nonclassical stationary shock at $x = 0$, i.e. assume $\rho(t, 0-) = \hat{\rho}_l^F$ and $\rho(t, 0+) = \check{\rho}_r^F$. In particular, we know that $f(\hat{\rho}_l^F) = f(\check{\rho}_r^F) = F$ and $\hat{\rho}_l^F > \check{\rho}_r^F$. Take now a non-negative test function $\xi \in \mathbf{C_c^1}((0, +\infty))$ and take $\varphi_\varepsilon = w_\varepsilon \xi$ with $\varepsilon > 0$ in (8). Here w_ε is the cut-off function defined by

$$w_\varepsilon(x) = \begin{cases} 1 & \text{if } |x| < \varepsilon, \\ 2 - |x|/\varepsilon & \text{if } \varepsilon \leq |x| \leq 2\varepsilon, \\ 0 & \text{if } |x| > 2\varepsilon. \end{cases} \quad (10)$$

Then the entropy inequality (8) becomes

$$I(\varepsilon)+J(\varepsilon)\geq 0,$$
$$I(\varepsilon)=\int_0^{+\infty}\int_{\mathbb{R}}\left(|\rho-\kappa|\partial_t\xi+\Phi(\rho,\kappa)\partial_x\xi\right)\,w_\varepsilon\,dx\,dt,$$
$$J(\varepsilon)=\int_0^{+\infty}\int_{\mathbb{R}}\Phi(\rho,\kappa)\xi w'_\varepsilon\,dx\,dtx+2\int_0^{+\infty}\left(f(\kappa)-f(\kappa)\perp F\right)\,\xi(t)\,dt.$$

Clearly, $\lim_{\varepsilon\to 0} I(\varepsilon)=0$. Moreover, using the definition of traces, we deduce

$$\lim_{\varepsilon\to 0} J(\varepsilon)=\int_0^{+\infty}\Big(\Phi(\rho(t,0-),\kappa)-\Phi(\rho(t,0+),\kappa)\\ +2\left(f(\kappa)-f(\kappa)\perp F\right)\Big)\,\xi(t)\,dt,$$

which gives for all $\kappa\in[0,1]$ and a.e. $t>0$ (dropping the time dependence)

$$\Phi(\rho^-,\kappa)-\Phi(\rho^+,\kappa)+2\left(f(\kappa)-f(\kappa)\perp F\right)\geq 0, \tag{11}$$

where we have set $\rho^\pm=\rho(t,0\pm)$. In our case, (11) writes

$$\Phi(\hat\rho_l^F,\kappa)-\Phi(\check\rho_r^F,\kappa)+2\left(f(\kappa)-f(\kappa)\perp F\right)\geq 0. \tag{12}$$

To check (12), let us consider the case $\check\rho_r^F\leq\kappa\leq\hat\rho_l^F$, so that the left hand side of (12) rewrites

$$\begin{aligned}&f(\hat\rho_l^F)-f(\kappa)-f(\kappa)+f(\check\rho_r^F)+2\left(f(\kappa)-f(\kappa)\perp F\right)\\&=2F-2f(\kappa)+2\left(f(\kappa)-f(\kappa)\perp F\right)\\&=2F-2f(\kappa)\perp F\geq 0.\end{aligned}$$

The cases $\kappa<\check\rho_r^F$ and $\kappa>\hat\rho_l^F$ can be checked in the same way.

Let us now check that other possible non-classical stationary discontinuities are ruled out by (8):

- Assume first that $\rho^->\rho^+$, $f(\rho^-)=f(\rho^+)=\tilde f<F$, and there exists $\bar\kappa\in[\rho^+,\rho^-]$ such that $f(\bar\kappa)>\tilde f$. In this case, (11) becomes, for $\rho^+\leq\kappa\leq\rho^-$,

  $$\begin{aligned}&f(\rho^-)-f(\kappa)-f(\kappa)+f(\rho^+)+2\left(f(\kappa)-f(\kappa)\perp F\right)\\&=2\tilde f-2f(\kappa)+2\left(f(\kappa)-f(\kappa)\perp F\right)\\&=2\tilde f-2f(\kappa)\perp F.\end{aligned}$$

  If we now choose $\kappa=\bar\kappa$, we get

  $$2\tilde f-2f(\bar\kappa)\perp F=2\left(\tilde f-f(\bar\kappa)\perp F\right)<0,$$

  hence the discontinuity is not admissible.
- We consider now the case where $\rho^-<\rho^+$, with $f(\rho^-)=f(\rho^+)=\tilde f\leq F$ and there exists $\bar\kappa\in[\rho(t,0-),\rho(t,0+)]$ such that $f(\bar\kappa)<\tilde f$. In this case, for $\rho(t,0-)\leq\kappa\leq\rho(t,0+)$, (11) becomes

  $$\begin{aligned}&f(\kappa)-f(\rho^-)-f(\rho^+)+f(\kappa)+2\left(f(\kappa)-f(\kappa)\perp F\right)\\&=2f(\kappa)-2\tilde f+2\left(f(\kappa)-f(\kappa)\perp F\right)\\&=4f(\kappa)-2\tilde f-2f(\kappa)\perp F.\end{aligned}$$

  Taking $\kappa=\bar\kappa$ in the above expression we get

  $$4f(\bar\kappa)-2\tilde f-2f(\bar\kappa)\perp F=2\left(f(\bar\kappa)-\tilde f\right)<0.$$

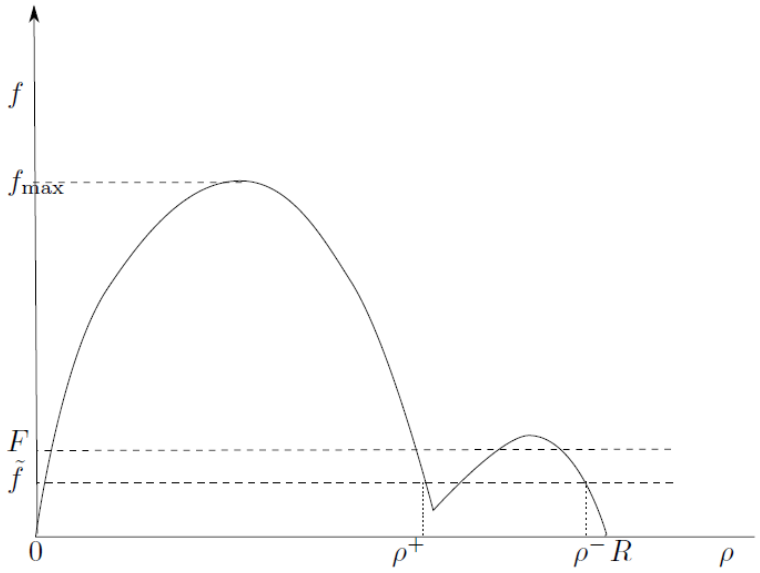

FIGURE 1. Example of traces at $x = 0$ that are not ruled out by condition [12, (3.2)]

To conclude the proof, it now suffices to write (8) with test function $\xi(1 - w_\varepsilon)$ (which gives a positive term since the solution is a classical entropy solution away from $x = 0$), add it to $I(\varepsilon) + J(\varepsilon)$ and pass to the limit as $\varepsilon \to 0$. □

Remark 2. Condition (8) differs in the last integrand from the entropy condition given in [12]. More precisely, the condition given here is finer, in the sense that (8) implies the inequality [12, (3.2)]. In fact it is straightforward to check that

$$f(\kappa) - f(\kappa) \perp F(t) \leq \left(1 - \frac{F(t)}{f_{\max}}\right) f(\kappa), \quad \text{for all } t > 0,\ \kappa \in [0, R].$$

Moreover, condition [12, (3.2)] does not work in the setting of non-concave fluxes, since it is not sufficient to rule out some non-maximal non-classical stationary shocks. In fact, let us consider for example the situation depicted in Fig. 1, where $\rho^- > \rho^+$, $f(\rho^-) = f(\rho^+) = \tilde{f}$, $F = \tilde{f} + \varepsilon$, for some $\varepsilon > 0$ small, and $f_{\max} \gg f(k)$ for all $k \in [\rho^+, \rho^-]$. Condition [12, (3.2)] would give

$$\Phi(\rho^-, \kappa) - \Phi(\rho^+, \kappa) + 2f(\kappa)\,(1 - F/f_{\max}) \geq 0$$

instead of (11), and taking $\kappa \in [\rho^+, \rho^-]$, the left-hand side of the above inequality would read in this case

$$\begin{aligned} 2\tilde{f} - 2f(\kappa) + 2f(\kappa)\,(1 - F/f_{\max}) &= 2\left(\tilde{f} - f(\kappa)F/f_{\max}\right) \\ &= \tilde{f}\,(1 - f(\kappa)/f_{\max}) - \varepsilon f(\kappa)/f_{\max}, \end{aligned}$$

which is positive for every $\kappa \in [\rho^+, \rho^-]$, if ε is taken sufficiently small. This shows that traces ρ^-, ρ^+ would have been admissible under condition [12, (3.2)], even if they satisfy the constraint with strict inequality, which we do not allow for non-classical shocks (this would prevent uniqueness of solutions).

Condition (8) was first found by the authors when passing to the limit in the discrete entropy inequality for finite volume approximations in the concave case (see the proof of [2, Proposition 4.7]). In that case, the two formulations turned out to be equivalent.

In order to formulate a second (equivalent) definition that does not need the explicit condition (9) on traces as in [2], and based on assumptions **(F.1)** - **(F.3.3)**, we introduce the following sets:

- $\mathcal{G}_1(F) = \{(c_l, c_r) \in [0,R]^2; c_l > c_r, f(c_l) = f(c_r) = F, \exists r \in [c_r, c_l]$ s.t. $f(r) > F\}$,
- $\mathcal{G}_2(F) = \{(c,c) \in [0,R]^2; f(c) \leq F\}$,
- $\mathcal{G}_3(F) = \{(c_l, c_r) \in [0,R]^2; f(c_l) = f(c_r) \leq F,\ (c^* - c_l)(f(c^*) - f(c_l)) \geq 0\ \forall c^* \in [c_l \perp c_r, c_l \top c_r]\}$,

and denote

$$\mathcal{G}(F) = \mathcal{G}_1(F) \cup \mathcal{G}_2(F) \cup \mathcal{G}_3(F).$$

Remark that the sets $\mathcal{G}_2$ and $\mathcal{G}_3$ contain the traces of classical entropy weak solutions (continuous parts or entropy admissible shocks), while $\mathcal{G}_1$ contains the traces of nonclassical discontinuities that can even result by superposition of classical and nonclassical shocks at zero speed. Globally, the set $\mathcal{G}$ contains nothing but the traces allowed by Definition 2.2, as stated by Lemma 2.4 below.

We also define the functions $c : \mathbb{R} \to [0,R]^2$ by

$$c(x) = \begin{cases} c_l & \text{if } x < 0, \\ c_r & \text{if } x > 0, \end{cases} \tag{13}$$

with $(c_l, c_r) \in [0,R]^2$.

Definition 2.3. A function $\rho \in \mathbf{L}^\infty(\mathbb{R}^+ \times \mathbb{R}; [0,R])$ is a weak entropy solution of (1)-(3) if there exists $M > 0$ such that for every $\varphi \in \mathbf{C_c^1}(\mathbb{R}^+ \times \mathbb{R}; \mathcal{R}^+)$ and all c defined by (13),

$$\begin{aligned} &\int_0^{+\infty} \int_{\mathbb{R}} (|\rho(t,x) - c(x)|\partial_t + \Phi(\rho(t,x), c(x))\partial_x)\ \varphi(t,x)\ dx\ dt \\ &+ \int_{\mathbb{R}} |\rho_0(x) - c(x)|\ \varphi(0,x)\ dx + M \int_0^{+\infty} \operatorname{dist}\left((c_l, c_r), \mathcal{G}(F(t))\right)\ \varphi(t,0)\ dt \geq 0. \end{aligned} \tag{14}$$

The above definition follows the more general approach based on admissibility germs presented in [3], and references therein. In particular, other definitions of the reminder term in (14) are possible. Here, we kept the notion of "distance" in accordance with [2].

Definitions 2.2 and 2.3 are equivalent. In fact we can prove the following

Proposition 2. *A function $\rho \in \mathbf{L}^\infty(\mathbb{R}^+ \times \mathbb{R}; [0,R])$ satisfies (8)-(9) if and only if it satisfies (14).*

The proof is detailed in [2, Proof of Proposition 2.6]. We only need to verify that [2, Lemma 2.7] still holds. We report it below for completeness, the proof being postponed to Section 5.

Lemma 2.4. [2, Lemma 2.7]
(i) If $(b_l, b_r) \in \mathcal{G}(F)$, then

$$\forall (c_l, c_r) \in \mathcal{G}(F), \quad \Phi(b_l, c_l) \geq \Phi(b_r, c_r). \tag{15}$$

(ii) The converse is true, under the following form:

$$\begin{array}{l} \textit{if (15) holds and the Rankine-Hugoniot condition} \\ f(b_l) = f(b_r) \textit{ is satisfied, then } (b_l, b_r) \in \mathcal{G}(F). \end{array} \tag{16}$$

To conclude this section, we state a well-posedness result for (1)-(3).

Theorem 2.5. *For any $\rho_0 \in \mathbf{L}^\infty(\mathbb{R}; [0, R])$ and $F \in \mathbf{L}^\infty(\mathbb{R}^+; [0, f_{\max}])$, there exists one and only one entropy solution $\rho \in \mathbf{L}^\infty(\mathbb{R}^+ \times \mathbb{R}; [0, R])$ to problem (1)-(3) (in the sense of Definitions 2.2 and 2.3). Moreover, assume $F^1, F^2 \in \mathbf{L}^\infty(\mathbb{R}^+; [0, f_{\max}])$, and $\rho_0^1, \rho_0^2 \in \mathbf{L}^\infty(\mathbb{R}, [0, R])$ such that $(\rho_0^1 - \rho_0^2) \in \mathbf{L}^1(\mathbb{R})$. Assume that ρ^1, ρ^2 are entropy solutions of (1)-(3), corresponding to the initial data ρ_0^1, ρ_0^2 and to the constraints F^1, F^2, respectively. Then, for a.e. $T > 0$, we have*

$$\int_{\mathbb{R}} |\rho^1 - \rho^2|(T, x)\, dx \;\leq\; 2 \int_0^T |F^1 - F^2|(t)\, dt \;+\; \int_{\mathbb{R}} |\rho_0^1 - \rho_0^2|(x)\, dx. \tag{17}$$

The proof of this theorem is postponed to Section 5.2.

3. **Finite volume numerical schemes for the constrained problem.** We now present a class of numerical schemes which easily account for the constraint (3). The idea is exactly the same as the one proposed in [2]. First of all, let us present some usual notations. We introduce a space step Δx and a time step Δt, both assumed to be constant, and we set $\nu = \Delta t / \Delta x$. We define the mesh interfaces $x_{j+1/2} = j\Delta x$ for $j \in \mathbb{Z}$ and the intermediate times $t^n = n\Delta t$ for $n \in \mathbb{N}$. At each time t^n, ρ_j^n represents an approximation of the mean value of the solution to (1)-(2) on the interval $[x_{j-1/2}, x_{j+1/2})$, $j \in \mathbb{Z}$. Therefore, a piecewise constant approximate solution $x \to \rho_\nu(x, t^n)$ is given by

$$\rho_\nu(x, t^n) = \rho_j^n \;\text{ for all }\; x \in C_j = [x_{j-1/2}, x_{j+1/2}[\;,\;\; j \in \mathbb{Z},\;\; n \in \mathbb{N}.$$

When $n = 0$, we set

$$\rho_j^0 = \frac{1}{\Delta x} \int_{x_{j-1/2}}^{x_{j+1/2}} \rho_0(x) dx, \;\text{ for all }\; j \in \mathbb{Z}.$$

In the case of classical conservation laws (1), a well-known class of finite volume approximation is defined by the so-called three-point monotone schemes:

$$\rho_j^{n+1} = \rho_j^n - \frac{\Delta t}{\Delta x}(f_{j+1/2}^n - f_{j-1/2}^n) \tag{18}$$

where $f_{j+1/2}^n = g(\rho_j^n, \rho_{j+1}^n)$ for any $j \in \mathbb{Z}$ and $n \in \mathbb{N}$, and g satisfies the following assumptions:

- Lipschitz continuity: $g \in \mathbf{W}^{1,\infty}([0, R]^2)$ with Lipschitz constant L_g.
- Consistency: $\forall a \in [0, R]$, $g(a, a) = f(a)$.
- Monotonicity: g is nondecreasing w.r.t. its first variable and nonincreasing w.r.t. its second variable.

Under the CFL condition

$$\nu \leq \frac{1}{2L_g}, \tag{19}$$

such a numerical scheme converges to the classical (Kružhkov [26]) entropy weak solution of (1), (2), see for example [20]. In [2], the authors proposed to modify such a scheme at the interface where the constraint (3) acts:

$$f_{1/2}^n = \min(g(\rho_0^n, \rho_1^n), F(t^n)), \tag{20}$$

keeping elsewhere

$$f^n_{j+1/2} = g(\rho^n_j, \rho^n_{j+1}) \quad \forall j \neq 0. \tag{21}$$

The most important remark is that the local modification of the numerical flux (20) does not affect the monotonicity of the scheme:

$$\begin{aligned} &\text{Under condition (19),} \\ &\rho^{n+1}_j \text{ is a nondecreasing function of } \rho^n_{j-1},\ \rho^n_j \text{ and } \rho^n_{j+1}. \end{aligned} \tag{22}$$

Therefore, we can easily deduce the $\mathbf{L}^\infty$ bound for the numerical scheme:

$$0 \leq \rho_\nu \leq R \quad \text{a.e.} \tag{23}$$

and, as a result of the Crandall-Tartar lemma [17], we have the discrete time continuity estimate (see [6]):

$$\sum_{j\in\mathbb{Z}} |\rho^{n+1}_j - \rho^n_j| \leq |\rho_0|_{\mathbf{BV}(\mathbb{R})}. \tag{24}$$

It is clear that it is very difficult to control the variation of the ρ_ν in the space direction due to the nontrivial treatment of the interface. However, one may follow the successful strategy developed in [6]. Using the estimate (24), it is possible to prove $\mathbf{BV}$ bounds far from the interface, let us say on $[-B,-A]\cup[A,B]$, with $0<A<B$. For almost any $T>0$, these take the form

$$|\rho_\nu(T,.)|_{\mathbf{BV}(A,B)} \leq |\rho_0|_{\mathbf{BV}(A,B)} + \frac{K}{r}, \tag{25}$$

where $0<r<A$ and for Δx sufficiently small (smaller than r). Though this bound blows up when $A\to 0$ (since $r\to 0$), convergence as $\Delta x\to 0$ can be achieved on $[-B,-A]\cup[A,B]$ for any fixed A by the Helly's theorem. Therefore, taking a decreasing sequence $(A_m)_m$ and letting Δx tend to 0 for each A_m, one may use the Cantor diagonal process to extract a subsequence to the numerical approximation which converges almost everywhere to a function of $\mathbf{L}^\infty(\mathbb{R}^+\times\mathbb{R})$.

Now we have to identify this limit. To do so, we derive the discrete entropy inequalities verified by the numerical scheme. Following [2], one may check that, for any $(k_j)_{j\in\mathbb{Z}}\subset[0,R]$, $j\in\mathbb{Z}$ and $n\in\mathbb{N}$,

$$|\rho^{n+1}_j - \kappa_j| - |\rho^n_j - \kappa_j| + \nu(F^n_{j+1/2} - F^n_{j-1/2}) - \nu H^n_i \leq 0 \tag{26}$$

where

$$F^n_{j+1/2} = \begin{cases} g(\rho^n_j \top \kappa_i, \rho^n_{j+1}\top\kappa_{j+1}) - g(\rho^n_j\perp\kappa_i, \rho^n_{j+1}\perp\kappa_{j+1}) & \text{if } j\neq 0 \\ \min(g(\rho^n_j\top\kappa_i,\rho^n_{j+1}\top\kappa_{j+1}), F(t^n)) & \\ \qquad - \min(g(\rho^n_j\perp\kappa_i,\rho^n_{j+1}\perp\kappa_{j+1}), F(t^n)) & \text{if } j=0 \end{cases}$$

and

$$H^n_i = \begin{cases} |\min(g(\kappa_0,\kappa_1), F(t^n)) - g(\kappa_{-1},\kappa_0)| & \text{if } j=0, \\ |g(\kappa_1,\kappa_2) - \min(g(\kappa_0,\kappa_1), F(t^n))| & \text{if } j=1, \\ 0 & \text{else.} \end{cases}$$

Starting form inequalities (26), one may use the proof of the Lax-Wendroff theorem to deduce that any limit $\bar\rho\in\mathbf{L}^\infty(\mathbb{R}^+\times\mathbb{R})$ of the numerical scheme satisfies for all

$(c_l, c_r) \in [0, R]^2$

$$\int_{\mathbb{R}^+} \int_{\mathbb{R}} (|\bar{\rho}(t,x) - c(x)|\partial_t + \Phi(\bar{\rho}(t,x), c(x))\partial_x)\ \varphi(t,x)\ dx\ dt + \int_{\mathbb{R}} |\rho_0(x) - c(x)|\ \varphi(0,x)\ dx + 12 L_g \int_{\mathbb{R}^+} \operatorname{dist}\left((c_l, c_r), \mathcal{G}_1(F(t)) \cup \mathcal{G}_2(F(t))\right)\ \varphi(t,0)\ dt \geq 0 \quad (27)$$

where c is defined by (13). The proof can be found in [2], but let us comment the last term. Actually, it attests to the fact that the scheme is able to preserve exactly any initial data $\rho_0(x) = c(x)$ with c given by (13) and $(c_l, c_r) \in \mathcal{G}_1(F) \cup \mathcal{G}_2(F)$, as soon as F is constant in t. For the case $(c_l, c_r) \in \mathcal{G}_3(F)$, which corresponds to a stationary shock wave, most of numerical schemes cannot preserve such initial data since they introduce numerical diffusion. The last step is now to prove that if $\bar{\rho}$ satisfies (27), then it also satisfies (14). Once again, the answer can be found in [2], Lemma 4.8.

Remark 3. In the case of a bell-shaped flux function f treated in [2], the authors prove the convergence of the numerical scheme to the entropy solution of (1)-(3). The proof relies on the use of constrained entropy-process solutions, which generalize the concept of entropy solution to Young measures. Morevoer, if the numerical flux g is the Godunov flux, it has been shown in [7] that error estimates can be obtained, on the basis of modified **BV** estimates. Here, though the numerical scheme is exactly the same, the extension of the analysis of convergence to constrained solutions associated with flux functions which comply with properties **(F.1)-(F.3.3)** is not straightforward. Therefore, we have used the strategy developed in [6], which allows us to avoid the study of measure-valued solutions (this method has been also used in a similar framework in [1]). The proof is much simpler and we have stated here only the main guidelines. Note, however, that the derivation of error estimates with these more complex flux functions is an open question, since the techniques of [7] are very dependent on the bell shape of f.

4. Application to pedestrian flow modeling.

The theory developed in the previous sections cannot be applied directly to the one-dimensional pedestrian flow model introduced by Colombo and Rosini [15], because of the presence of non-classical solutions, which are the characteristic feature of the model. Therefore, the definition of constraint-satisfying solutions has to be adapted to the non-classical Riemann solver, whose description is recalled in Section 4.1.

Due to the presence of non-classical discontinuities, beside the stationary one caused by the flux constraint, entropy conditions and uniqueness results are not available in this framework. In fact, $\mathbf{L^1}$-stability does not hold even in the unconstrained setting, see [16, Prop. 3.6] and [31, Prop. 3.3]. Nevertheless, the well-posedness result proved in Section 2.2 still holds if no panic arises. Moreover, the numerical techniques developed in Section 3 prove to be useful for the construction of a numerical scheme capable to deal with flux constraint even in the presence of non-classical waves, as detailed in Sections 4.4 and 4.5.

4.1. A non-classical Riemann solver.

The model of pedestrian traffic flow introduced in [15, 16] is based on a flux function f like the one represented in Figure 2.

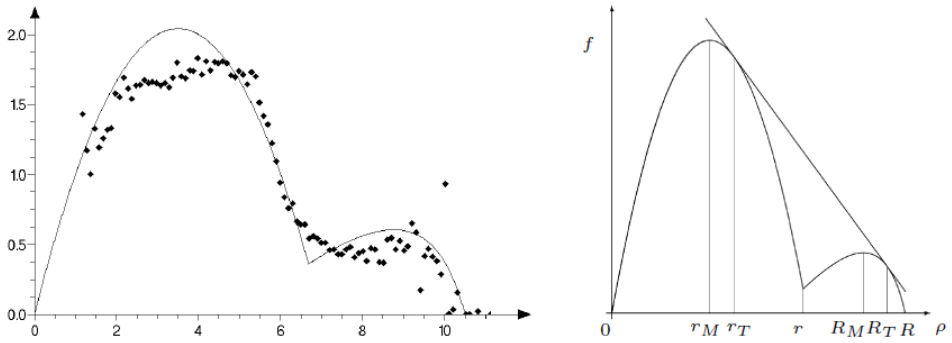

FIGURE 2. Left, a flow satisfying hypotheses in [16]. Superimposed are experimental measurements from [24]. Crowd density, ρ, is on the horizontal axis and flow, ρv, on the vertical one. Right, notations used in the paper. (Figures taken from [13, 16].)

In particular, f has a local minimum at r, which is the maximal density in normal (non-panic) situations, while bigger densities $r < \rho \leq R$ can be reached in case of panic.

For simplicity, it is assumed that the restrictions $f_{|[0,r]}$ and $f_{|[r,R]}$ are strictly concave. Hence there exists a unique point $r_M \in]0, r[$ such that

$$f(r_M) = \max\{f(\rho)\colon \rho \in [0, r]\}$$

and a unique point $R_M \in]r, R[$ such that

$$f(R_M) = \max\{f(\rho)\colon \rho \in [r, R]\}.$$

The evolution of the solutions to (1) is governed through the introduction of non-entropic shocks, which violate the maximum principle and then allow the appearance of panic from non-panic regimes.

As it is usual when dealing with non-classical scalar conservation laws, see [27, Chapter II], in [15] authors introduced the auxiliary functions ψ and φ, see Figure 3, left.

Let $\psi(r) = r$ and, for $\rho \neq r$, let $\psi(\rho)$ be such that the straight line through $(\rho, f(\rho))$ and $(\psi(\rho), f \circ \psi(\rho))$ is tangent to the graph of f at $(\psi(\rho), f \circ \psi(\rho))$. Let $r_T \in]0, r[$ and $R_T \in]r, R[$ be such that $\psi(r_T) = R_T$ and $\psi(R_T) = r_T$ (see Fig. 2, right). Besides, for $\rho \in [0, r_T[$, the line through $(\rho, f(\rho))$ and $(\psi(\rho), f \circ \psi(\rho))$ has a further intersection with the graph of f, which we call $(\varphi(\rho), f \circ \varphi(\rho))$. In [15], the authors introduce two thresholds s and Δs such that

$$s > 0\,,\ \Delta s > 0\,,\ s < r_M \text{ and } r > s + \Delta s \geq \varphi(s) > r_T > r - \Delta s\,. \tag{28}$$

Here we will also assume that

$$f(s) > f(r).$$

The nonclassical Riemann solver $\mathcal{R}_{NC}$ is then defined as follows. Let

$$\mathcal{NS}(\rho_l, \rho_r)(\lambda) = \begin{cases} \rho_l & \text{if } \lambda < \Lambda(\rho_l, \rho_r), \\ \rho_r & \text{if } \lambda > \Lambda(\rho_l, \rho_r), \end{cases}$$

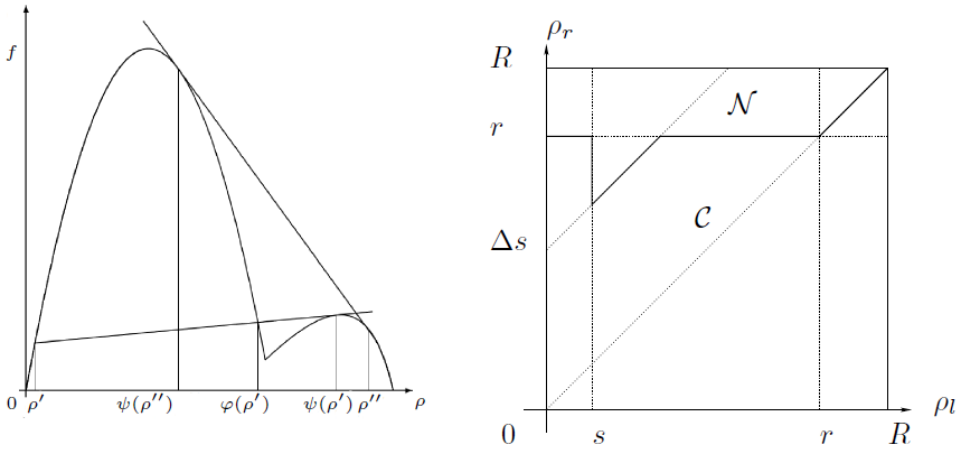

FIGURE 3. Left, the functions ψ and φ: their geometrical meaning. Right, the Riemann Solver: in $\mathcal{C}$, the solution consists of classical waves only; in $\mathcal{N}$, also non-classical shocks are present.

denote the non-entropic jump joining ρ_l to ρ_r and moving with the speed given by the Rankine-Hugoniot equation

$$\Lambda(\rho_l, \rho_r) = \frac{f(\rho_l) - f(\rho_r)}{\rho_l - \rho_r}.$$

- If $\rho_l, \rho_r \in [0, r]$ and $\rho_l > s,\ \rho_r - \rho_l > \Delta s$, then

$$\mathcal{R}_{NC}(\rho_l, \rho_r)(\lambda) = \begin{cases} \mathcal{NS}(\rho_l, \psi(\rho_l))(\lambda) & \text{if } \lambda < f'(\psi(\rho_l)), \\ \mathcal{R}(\psi(\rho_l), \rho_r) & \text{if } \lambda > f'(\psi(\rho_l)). \end{cases}$$

- If $\rho_l < r < \rho_r$ and the segment between $(\rho_l, f(\rho_l))$ and $(\rho_r, f(\rho_r))$ intersects the curve $f = f(\rho)$, then

$$\mathcal{R}_{NC}(\rho_l, \rho_r)(\lambda) = \begin{cases} \mathcal{NS}(\rho_l, \psi(\rho_l))(\lambda) & \text{if } \lambda < f'(\psi(\rho_l)), \\ \mathcal{R}(\psi(\rho_l), \rho_r) & \text{if } \lambda > f'(\psi(\rho_l)), \end{cases}$$

  if $\rho_r < \psi(\rho_l)$, and

$$\mathcal{R}_{NC}(\rho_l, \rho_r) = \mathcal{NS}(\rho_l, \rho_r)$$

  if $\rho_r \geq \psi(\rho_l)$.
- Otherwise, $\mathcal{R}_{NC}(\rho_l, \rho_r) = \mathcal{R}(\rho_l, \rho_r)$.

4.2. **The constrained non-classical Riemann solver.** As in Section 2.1, we construct the constrained Riemann solver derived from $\mathcal{R}_{NC}$.

Definition 4.1. A Riemann solver $\mathcal{R}^F_{NC} : (\rho_l, \rho_r) \mapsto \mathcal{R}^F_{NC}(\rho_l, \rho_r)$ for (1)-(3) is defined as follows.
If $f\left(\mathcal{R}_{NC}(\rho_l, \rho_r)(0)\right) \leq F$, then $\mathcal{R}^F_{NC}(\rho_l, \rho_r) = \mathcal{R}_{NC}(\rho_l, \rho_r)$.
Otherwise, if $s < \rho_l < r$ and $\hat{\rho}^F_l > \rho_l + \Delta s$ then

$$\mathcal{R}^F_{NC}(\rho_l, \rho_r)(\lambda) = \begin{cases} \mathcal{R}_{NC}(\rho_l, \hat{R}^F_M)(\lambda) \text{ if } \lambda < 0\,, \\ \mathcal{R}_{NC}(\check{\rho}^F_r, \rho_r)(\lambda) \text{ if } \lambda > 0\,. \end{cases}$$

In all the other cases

$$\mathcal{R}^F_{NC}(\rho_l,\rho_r)(\lambda)=\left\{\begin{array}{l}\mathcal{R}_{NC}(\rho_l,\hat\rho_l^F)(\lambda)\ \text{if}\ \lambda<0\,,\\ \mathcal{R}_{NC}(\check\rho_r^F,\rho_r)(\lambda)\ \text{if}\ \lambda>0\,.\end{array}\right.$$

In order to check that the above definition is correct, observe first of all that if $f(\rho_l)\le F$, then $\hat\rho_l^F\le\rho_l$ and consequently $\mathcal{R}_{NC}(\rho_l,\hat\rho_l^F)=\mathcal{R}(\rho_l,\hat\rho_l^F)$, falling in the setting of Definition 2.1. Similarly, if $f(\rho_r)\le F$, then $\check\rho_r^F\ge\rho_r$ and consequently $\mathcal{R}_{NC}(\check\rho_r^F,\rho_r)=\mathcal{R}(\check\rho_r^F,\rho_r)$

Consider now the case $f(\rho_l)>F$. We have to distinguish three cases:

- If $F\in\,]f(R_M),f(r_M)]$, then $\mathcal{R}_{NC}(\rho_l,\hat\rho_l^F)=\mathcal{R}(\rho_l,\hat\rho_l^F)$.
- If $F\in[f(r),f(R_M)]$, and moreover $\rho_l>s$, $\hat\rho_l^F>\rho_l+\Delta s$, then $\mathcal{R}_{NC}(\rho_l,\hat\rho_l^F)$ would contain positive waves, and would not satisfy the constraint (9). On the contrary, $\mathcal{R}_{NC}(\rho_l,\hat R_M^F)=\mathcal{NS}(\rho_l,\hat R_M^F)$ consists of a shock with negative speed. In all the other cases, we have $\mathcal{R}_{NC}(\rho_l,\hat\rho_l^F)=\mathcal{R}(\rho_l,\hat\rho_l^F)$.
- If $F\in[0,f(r)[$, $\mathcal{R}_{NC}(\rho_l,\hat\rho_l^F)$ contains only waves with negative speeds.

We now check the right hand side of the Riemann solver, i.e. for $\lambda>0$, and $f(\rho_r)>F$. We distinguish two cases:

- If $F\in[f(r),f(r_M)]$, then $\mathcal{R}_{NC}(\check\rho_r^F,\rho_r)=\mathcal{R}(\check\rho_r^F,\rho_r)$.
- If $F\in[0,f(r)[$, then $\mathcal{R}_{NC}(\check\rho_r^F,\rho_r)$ contains only waves with positive speeds.

Note that non-classical shocks can appear both in $\mathcal{R}_{NC}(\rho_l,\hat\rho_l^F)$ and $\mathcal{R}_{NC}(\check\rho_r^F,\rho_r)$ as, for example, if $F<f(r)$, $\rho_l\in[0,r_M]$ with $f(\rho_l)>F$ and $\rho_r\in[r,R_M]$ (which implies $f(\rho_r)>F$).

4.3. **A numerical scheme for classical and non-classical solutions.** We propose here a numerical scheme for computing classical and nonclassical solutions of (1)-(2), which follows the same "sharp-interface approach" as in [8, 9]. It is made of two steps. The first step tracks the (classical or non-classical) discontinuities arising in the Riemann problems set at the mesh interfaces. The second step consists of a random sampling strategy in order to avoid dealing with moving meshes.

Let us first define the set $\mathcal{N}\in[0,R]^2$ made of the pairs (ρ_l,ρ_r) such that the Riemann solution $\mathcal{R}_{NC}(\rho_l,\rho_r)$ is actually non-classical, that is to say contains a non-classical shock. Similarly, we define the set $\mathcal{C}\in[0,R]^2$ made of the pairs (ρ_l,ρ_r) such that the Riemann solution $\mathcal{R}_{NC}(\rho_l,\rho_r)$ is made of classical waves. (See Fig. 3, right.)

Let us now present the numerical scheme for classical and non-classical solutions. We keep the notation of Section 3 and, being given the sequence $(\rho_j^n)_{j\in\mathbb{Z}}$ at time t^n, the point is now to propose a definition of $(\rho_j^{n+1})_{j\in\mathbb{Z}}$ by a recurrence relation.

Step 1: Tracking the discontinuities and averaging ($t^n\to t^{n+1-}$) The idea of this step is to first track the non-classical or classical discontinuities in the Riemann problems set at each mesh interface, and then to average the solution on both sides of these discontinuities.

As is customary in the classical Godunov method, one first solves theoretically the Cauchy problem (1)-(2) with $\rho_0(x)=\rho_\nu(x,t^n)$ for times $t\in[0,\Delta t]$. Under the usual CFL restriction

$$\frac{\Delta t}{\Delta x}\max_\rho\{|f'(\rho)|\}\le\frac12,\tag{29}$$

for all the ρ under consideration, the solution is known by gluing together the solutions of the Riemann problems set at each interface. More precisely

$$\rho(x,t) = \mathcal{R}_{NC}(\rho_j^n, \rho_{j+1}^n)\left(\frac{x - x_{j+1/2}}{t}\right) \quad \forall (x,t) \in [x_j, x_{j+1}] \times [0, \Delta t], \tag{30}$$

where $x_j = \dfrac{x_{j-1/2} + x_{j+1/2}}{2}$.

In order to track the discontinuities, we then define the sequence

$$(\sigma_{j+1/2}^n = \sigma(\rho_j^n, \rho_{j+1}^n))_{j\in\mathbb{Z}}$$

of characteristic speeds of propagation at interfaces $(x_{j+1/2})_{j\in\mathbb{Z}}$ as follows :

- if (ρ_j^n, ρ_{j+1}^n) belongs to $\mathcal{N}$, then $\sigma_{j+1/2}^n$ coincides with the speed of propagation of the non-classical discontinuity in the Riemann solution $\mathcal{R}_{NC}(\rho_j^n, \rho_{j+1}^n)$;
- if (ρ_j^n, ρ_{j+1}^n) belongs to $\mathcal{C}$, then $\sigma_{j+1/2}^n$ coincides with the speed of propagation of the classical discontinuity in the Riemann solution $\mathcal{R}_{NC}(\rho_j^n, \rho_{j+1}^n)$, if any;
- otherwise, $\sigma_{j+1/2}^n = 0$.

Assuming that, for all $j \in \mathbb{Z}$, the interface $x_{j+1/2}$ moves at velocity $\sigma_{j+1/2}^n$ between times t^n and $t^{n+1} = t^n + \Delta t$, it is natural to define the new interface $\overline{x}_{j+1/2}^n$ at time t^{n+1} by

$$\overline{x}_{j+1/2}^n = x_{j+1/2} + \sigma_{j+1/2}^n \, \Delta t, \quad j \in \mathbb{Z}. \tag{31}$$

We also introduce the notation $\overline{\Delta x}_j^n = \overline{x}_{j+1/2}^n - \overline{x}_{j-1/2}^n$, $j \in \mathbb{Z}$.

At last, averaging the solution on $\overline{\mathcal{C}}_j^n = [\overline{x}_{j-1/2}^n, \overline{x}_{j+1/2}^n[$ provides us with a piecewise constant approximate solution $\overline{\rho}_\nu(x, t^{n+1}-)$ on a non uniform mesh defined by

$$\overline{\rho}_\nu(x, t^{n+1}-) = \overline{\rho}_j^{n+1-} \quad \text{for all } \; x \in \overline{C}_j^n, \;\; j \in \mathbb{Z}, \;\; n \in \mathbb{N},$$

with

$$\overline{\rho}_j^{n+1-} = \frac{1}{\overline{\Delta x}_j^n} \int_{\overline{x}_{j-1/2}^n}^{\overline{x}_{j+1/2}^n} \rho(x, \Delta t) dt, \;\; j \in \mathbb{Z}.$$

It is worth noticing that the modified cells $\overline{\mathcal{C}}_j^n$ may be either smaller or larger than the original ones $\mathcal{C}_j$, depending on the signs of the velocities $\sigma_{j+1/2}^n$, $j \in \mathbb{Z}$. This is illustrated on Figures 4 and 5 below.

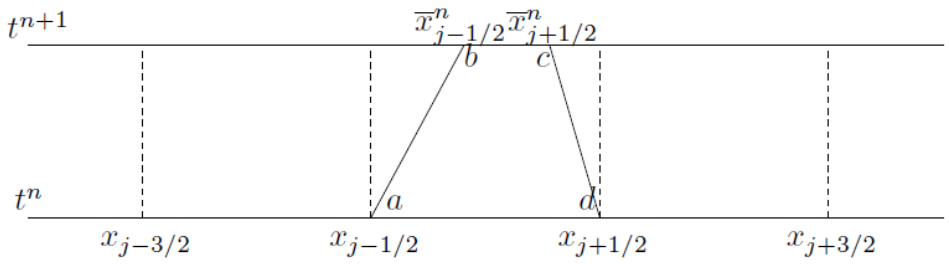

FIGURE 4. A first example of modified cells tracking the discontinuities.

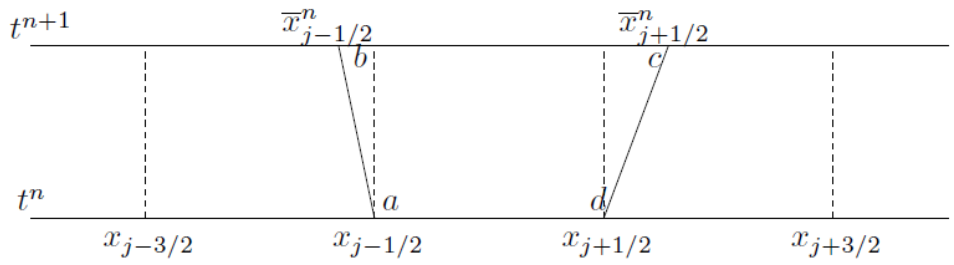

FIGURE 5. A second example of modified cells tracking the discontinuities.

Actually, using notations introduced on Figures 4 and 5 and integrating (1) over the element $\overline{E} = (abcd)$ with use of Green's theorem, we classically obtain the simpler formula

$$\overline{\rho}_j^{n+1-} = \frac{\Delta x}{\overline{\Delta x}_j^n}\rho_j^n - \frac{\Delta t}{\overline{\Delta x}_j^n}(\overline{\mathbf{f}}_{j+1/2}^{n,-} - \overline{\mathbf{f}}_{j-1/2}^{n,+}) \text{ for all } j \in \mathbb{Z}. \tag{32}$$

The numerical fluxes are defined by

$$\overline{f}_{j+1/2}^{n,\pm} = f\left(\mathcal{R}_{NC}(\rho_j^n, \rho_{j+1}^n)(\sigma_{j+1/2}^{n,\pm})\right) - \sigma_{j+1/2}^n \mathcal{R}_{NC}(\rho_j^n, \rho_{j+1}^n)(\sigma_{j+1/2}^{n,\pm}), \tag{33}$$

for all $j \in \mathbb{Z}$ where we have used the usual notations $\sigma_{j+1/2}^{n,\pm}$ to denote the left and right traces of the Riemann solver at $\lambda = \sigma_{j+1/2}^n$.

Remark. The conservation property

$$\begin{array}{c} f\left(\mathcal{R}_{NC}(\rho_j^n, \rho_{j+1}^n)(\sigma_{j+1/2}^{n,-})\right) - \sigma_{j+1/2}^n \mathcal{R}_{NC}(\rho_j^n, \rho_{j+1}^n)(\sigma_{j+1/2}^{n,-}) \\ = \\ f\left(\mathcal{R}_{NC}(\rho_j^n, \rho_{j+1}^n)(\sigma_{j+1/2}^{n,+})\right) - \sigma_{j+1/2}^n \mathcal{R}_{NC}(\rho_j^n, \rho_{j+1}^n)(\sigma_{j+1/2}^{n,+}) \end{array} \tag{34}$$

remains valid thanks to Rankine-Hugoniot conditions.

We finally introduce the notation $\overline{f}^{\pm}(\rho_j^n, \rho_{j+1}^n) = \overline{f}_{j+1/2}^{n,\pm}$ for the numerical fluxes, with of course

$$\overline{f}^{\pm}(\rho_j^n, \rho_{j+1}^n) = f\left(\mathcal{R}_{NC}(\rho_j^n, \rho_{j+1}^n)(\sigma_{j+1/2}^{n,\pm})\right) - \sigma_{j+1/2}^n \mathcal{R}_{NC}(\rho_j^n, \rho_{j+1}^n)(\sigma_{j+1/2}^{n,\pm}). \tag{35}$$

Recall that $\sigma_{j+1/2}^n = \sigma(\rho_j^n, \rho_{j+1}^n)$ by definition.

To conclude this first step, let us emphasize that when the Riemann solution between ρ_j^n and ρ_{j+1}^n does not present discontinuities, then $\sigma_{j+1/2}^n = 0$ and the numerical fluxes $\overline{f}_{j+1/2}^{n,\pm}$ coincide with the usual numerical flux

$$\overline{f}(\rho_j^n, \rho_{j+1}^n) = f\left(\mathcal{R}_{NC}(\rho_j^n, \rho_{j+1}^n)(0)\right)$$

associated with the Godunov method. This numerical flux may of course be replaced by any consistent numerical flux for the sake of simplicity. In the proposed numerical simulation below, we replaced for instance this Godunov numerical flux by the Rusanov numerical flux as soon as the solution joining ρ_j^n to ρ_{j+1}^n does not display discontinuities. This amounts to set

$$\overline{f}(\rho_j^n, \rho_{j+1}^n) = \frac{1}{2}\big(f(\rho_j^n) + f(\rho_{j+1}^n) - \alpha_{j+1/2}(\rho_{j+1}^n - \rho_j^n)\big), \tag{36}$$

with

$$\alpha_{j+1/2} = \max\left(f'(\rho_j^n), f'(\rho_{j+1}^n)\right).$$

Step 2 : Random sampling ($t^{n+1-} \to t^{n+1}$) In order to avoid dealing with moving meshes, we propose to define the new approximation ρ_j^{n+1} at time t^{n+1} on the (uniform) cells $\mathcal{C}_j$, $j \in \mathbb{Z}$, using a random sampling strategy. More precisely, we propose to pick up randomly a value between $\overline{\rho}_{j-1}^{n+1-}$, $\overline{\rho}_j^{n+1-}$ and $\overline{\rho}_{j+1}^{n+1-}$, according to their rate of presence in the cell $\mathcal{C}_j$. Given a well distributed random sequence (a_n) in the interval $]0,1[$, this leads to set:

$$\rho_j^{n+1} = \begin{cases} \overline{\rho}_{j-1}^{n+1-} & \text{if} \quad a_{n+1} \in (0, \frac{\Delta t}{\Delta x} \max(\sigma_{j-1/2}^n, 0)), \\ \overline{\rho}_j^{n+1-} & \text{if} \quad a_{n+1} \in [\frac{\Delta t}{\Delta x} \max(\sigma_{j-1/2}^n, 0), 1 + \frac{\Delta t}{\Delta x} \min(\sigma_{j+1/2}^n, 0)), \\ \overline{\rho}_{j+1}^{n+1-} & \text{if} \quad a_{n+1} \in [1 + \frac{\Delta t}{\Delta x} \min(\sigma_{j+1/2}^n, 0), 1), \end{cases} \tag{37}$$

for all $j \in \mathbb{Z}$.

Following Colella [11], we consider in practice the low-discrepancy van der Corput random sequence (a_n) defined by

$$a_n = \sum_{k=0}^{m} i_k 2^{-(k+1)},$$

where $n = \sum_{k=0}^{m} i_k 2^k$, $i_k = 0, 1$, denotes the binary expansion of the integers $n = 1, 2, \ldots$. This concludes the description of the modified Godunov scheme.

To conclude this section, it is worth emphasizing that, due to the sampling procedure, the proposed algorithm is not strictly conservative in the classical sense of finite volumes methods. However, we observed that this drawback does not prevent the approximate solutions to converge to the right one (see also for instance [8, 9]). In particular, discontinuities propagate with the right speed and conservation errors tend to zero with the mesh size. On the other hand, it is easily seen that if we focus on initial data leading to a solution that consists of an isolated (classical or non-classical) discontinuity, the proposed method coincides with the Glimm's random choice scheme and then converges to the exact solution.

4.4. **A numerical scheme for constrained classical and non-classical solutions.** We propose to describe in this section how to deal with constrained solutions. In practice and as motivated in the previous section, such constraints will appear at the exit of a corridor and possibly at suitable obstacles like columns posed before the exit of the corridor in order to lessen the crowd pressure. In this paragraph, we denote by $x_{j_c+1/2} = (j_c + 1/2)\Delta x$ the mesh interface associated with the position where such a constraint takes place (that is typically the position of the exit or of an obstacle).

In the framework of the numerical scheme proposed for non-constrained classical and nonclassical solutions in the previous subsection, first of all we have to define $\sigma_{j_c+1/2}^n$ and the corresponding numerical fluxes $\overline{f}_{j_c+1/2}^{n,\pm} = \overline{f}^{\pm}(\rho_{j_c}^n, \rho_{j_c+1}^n)$. Since the non-classical shock possibly arising because of the constraint is stationary, we set $\sigma_{j_c+1/2}^n = 0$ and we define the numerical flux at the interface $x_{j_c+1/2}$ as in Section 3 by the following constrained formula

$$\overline{f}_{j_c+1/2}^{n,\pm} = \overline{f}^{\pm}(\rho_{j_c}^n, \rho_{j_c+1}^n) = \min\left(\overline{f}(\rho_{j_c}^n, \rho_{j_c+1}^n), F\right),$$

where F represents the flux constraint and $\overline{f}(\rho_{j_c}^n, \rho_{j_c+1}^n)$ is given by the Rusanov formula (36).

We face two possibilities. The first one corresponds to the non-constrained situation $\overline{f}^{\pm}(\rho^n_{j_c},\rho^n_{j_c+1}) = \overline{f}(\rho^n_{j_c},\rho^n_{j_c+1}) < F$, where we use the classical Rusanov numerical flux. The second one corresponds to the constrained situation $\overline{f}^{\pm}(\rho^n_{j_c},\rho^n_{j_c+1}) = F$. In that case, the numerical flux is given by the constraint itself. From the theoretical point of view, a stationary discontinuity is expected to take place between the left and right states given by

$$(\rho^-_{j_c+1/2},\rho^+_{j_c+1/2}) = \begin{cases} (\hat{R}^F_M,\check{\rho}^{nF}_{j_c+1}) & \text{if } s<\rho^n_{j_c}<r \text{ and } \hat{\rho}^{nF}_{j_c}>\rho^n_{j_c}+\Delta s,\\ (\hat{\rho}^{nF}_{j_c},\check{\rho}^{nF}_{j_c+1}) & \text{otherwise,}\end{cases}$$

see Definitions 2.1 and 4.1 of the constrained classical and nonclassical Riemann solvers.

In order to take into account this theoretical statement at the numerical level, we propose to modify also the definition of the numerical fluxes $\overline{f}^{n,\pm}_{j_c-1/2}$ and $\overline{f}^{n,\pm}_{j_c+3/2}$ by setting

$$\overline{f}^{n,\pm}_{j_c-1/2} = \overline{f}^{\pm}(\rho^n_{j_c-1},\rho^-_{j_c+1/2})$$

and

$$\overline{f}^{n,\pm}_{j_c+3/2} = \overline{f}^{\pm}(\rho^+_{j_c+1/2},\rho^n_{j_c+2}),$$

with $\overline{f}^{\pm}(.,.)$ defined above by (35).

4.5. **Numerical experiment and Braess paradox.** As an illustrative simulation, we perform the so-called Braess paradox numerical experiment described below. Following [13, 16], we consider a corridor modeled by the segment $[0,L]$, with an exit at $x=D$, with $0<D<L$. Then, the dynamics of the crowd exiting the corridor is described by (1)-(3), with the Riemann solver described in Section 4.1. In emergency situations, it is well known that the pressure of the people seeking to exit may dramatically reduce the door efficiency. To prevent this, suitable obstacles (such as columns) can be posed before the exit to reduce the crowd pressure. Paradoxically, the insertion of obstacles may reduce the evacuation time, although most individuals may have a slightly longer path to reach the exit. This remarkable behavior mimics the Braess paradox [4] typical of networks and is captured by the model considered here.

We assume that a group of people is uniformly distributed on the segment $[a,b]$, with $0<a<b<D$, and an obstacle is placed at $x=d$, with $b<d<D$, see Figure 6.

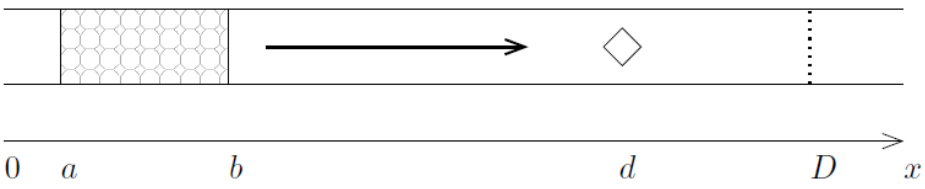

FIGURE 6. A corridor with an obstacle before the exit.

The dynamic of the crowd is then described by

$$\begin{cases} \partial_t\rho+\partial_x f(\rho)=0 & f\left(\rho(t,d-)\right) \le q\left(\rho(t,d-)\right),\\ \rho(0,x)=\rho_o(x) & f\left(\rho(t,D-)\right) \le Q\left(\rho(t,D-)\right).\end{cases} \tag{38}$$

Since it is well known that exit capacity is reduced in panic situations, we assume that

$$
\begin{aligned}
q(\rho) &= \begin{cases} \hat{q} & \text{if} \quad \rho \in [0, r] \\ \check{q} & \text{if} \quad \rho \in]r, R] \end{cases} \qquad \text{with} \quad \hat{q} > \check{q}, \\
Q(\rho) &= \begin{cases} \hat{Q} & \text{if} \quad \rho \in [0, r] \\ \check{Q} & \text{if} \quad \rho \in]r, R] \end{cases} \qquad \text{with} \quad \hat{Q} > \check{Q}.
\end{aligned}
\tag{39}
$$

Aiming at pedestrian flow management and exits design, the evacuation time T is particularly relevant and can be computed integrating (38)–(39) numerically following the procedure described in Sections 4.3 and 4.4 below. If the initial datum is particularly simple, i.e. constant on a given segment, an analytical study is also possible, see Figure 7.

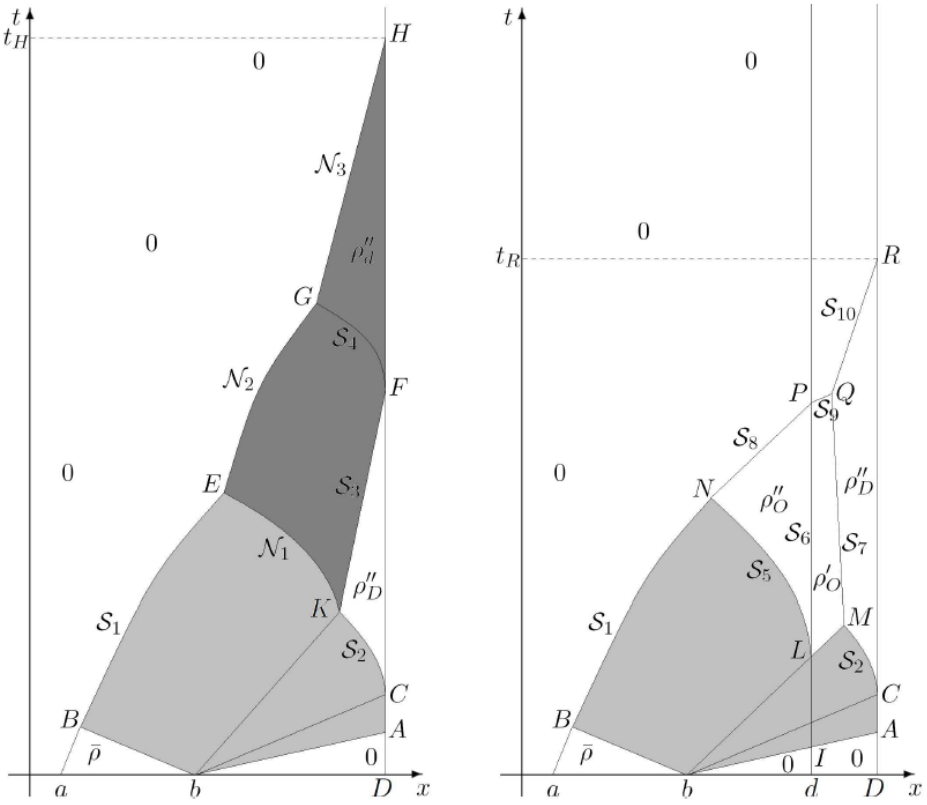

FIGURE 7. Wave-front tracking applied to (38)–(39). Left, the structure of the solution without obstacle ($q \geq \max(f(\rho))$): the evacuation time is t_H. Right, in the presence of the obstacle, the evacuation time is $t_R < t_H$. (Taken from [13, 16].)

The detailed construction of these solutions can be found in [16, Section 4.2]. Note that the darker regions in Figure 7, left, represent the regions where the crowd density attains panic values, i.e. $\rho \in]r, R]$. The presence of the obstacle avoids the density to reach panic regimes, thus allowing for a faster evacuation of the room.

The simulation parameters have been chosen as follows. We have considered the flow function [16, Section 4.3]

$$f(\rho) = \max\left\{\frac{\rho(7-\rho)}{6}, \frac{3(\rho-6)(2\rho-21)}{20(\rho-12)}\right\},$$

whose diagram is given in Figure 2 (left), leading to

$$r \approx 6.842786, \quad R = 10.5.$$

The nonclassical Riemann solver parameters are given by

$$s = 1.2, \quad \Delta_s = 5.6.$$

The computational domain modeling the corridor corresponds to the interval $[0, L]$ with $L = 3.6$, and the the exit is located at $x = D$ with $D = 3.1$. The position of the obstacle (when present) is $d = 2.45$. The initial datum is chosen to be

$$\rho_0(x) = \begin{cases} 0 & \text{if} \quad x < a = 0.1 \quad \text{and} \quad x > b = 1.1 \\ 5.3 & \text{if} \quad a < x < b, \end{cases}$$

and is represented on Figure 8 below.

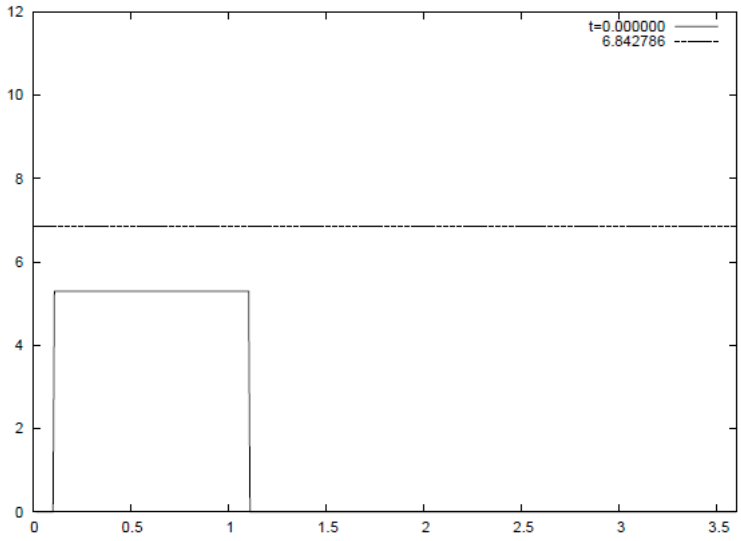

FIGURE 8. Braess paradox simulation : initial data

The constraint functions q and Q in (39) are considered with the following parameters :

$$\hat{q} = 1, \quad \hat{Q} = 0.2, \quad \check{Q} = 0.1793.$$

Note that the constraint function q is not active when the obstacle is not present while the parameter $\check{q}$ entering its definition does not play any role since no panic will be observed at the obstacle position. Note also that, from a numerical point of view, these flux constraints are imposed at both interfaces $j_c + 1/2$ associated with the obstacle and exit positions. The left traces $d-$ and $D-$ of the density in (38) are then naturally considered to be ρ_{j_c}.

We show here the results of two simulations, one without obstacle and one with obstacle, where we used a 500-point mesh and a CFL condition equal to 0.5. We

propose on Figure 9 four snapshots of each numerical solution. The numerical results without obstacle are depicted on the left side and we clearly see on the second picture that panic arises as expected since the density gets greater than r near the exit position. The numerical exit time is $t = 28.833$. On the contrary, no panic is created when the obstacle is present and the computed exit time now equals $t = 24.883$.

5. **Proofs.**

5.1. **Proof of Lemma 2.4.**

(i) We want to check that

$$\forall (c_l, c_r), (b_l, b_r) \in \mathcal{G}(F) \quad \Phi(c_l, b_l) \geq \Phi(c_r, b_r). \tag{40}$$

- If $(c_l, c_r), (b_l, b_r) \in \mathcal{G}_1(F)$, then $f(c_l) = f(c_r) = f(b_l) = f(b_r) = F$ and $\Phi(c_l, b_l) = 0 = \Phi(c_r, b_r)$.
- If $(c^l, c^r) \in \mathcal{G}_1(F)$, $(b^l, b^r) \in \mathcal{G}_2(F)$ (then $b_l = b_r = b$ and $f(b) \leq F$). In this case, either $F \in [0, f(r)[\cup]f(R_M^*), f(R_M)]$ and $\mathcal{G}_1(F) = \left\{(\rho_2^F, \rho_1^F)\right\}$, or $F \in [f(r), f(R_M^*)]$ and

  $$\mathcal{G}_1(F) = \left\{(\rho_4^F, \rho_1^F), (\rho_4^F, \rho_2^F), (\rho_4^F, \rho_3^F), (\rho_3^F, \rho_1^F), (\rho_2^F, \rho_1^F)\right\}.$$

  We have to check several cases. If $b \leq \rho_1^F$, then

  $$\Phi(c_l, b) - \Phi(c_r, b) = f(c_l) - f(b) - f(c_r) + f(b) = 0.$$

  If $b \geq \max_i\{\rho_i^F\}$, then again

  $$\Phi(c_l, b) - \Phi(c_r, b) = f(b) - f(c_l) - f(b) + f(c_r) = 0.$$

  If $\rho_2^F < b < \rho_3^F$, then we may have $c_r < b < c_l$ and

  $$\Phi(c_l, b) - \Phi(c_r, b) = f(c_l) - f(b) - f(b) + f(c_r) = 2F - 2f(b) \geq 0.$$

- If $(c_l, c_r) \in \mathcal{G}_1(F)$, $(b_l, b_r) \in \mathcal{G}_3(F)$, then we can face several situations. If $b_l \leq c_r < c_l \leq b_r$, then

  $$\Phi(c_l, b_l) - \Phi(c_r, b_r) = f(c_l) - f(b_l) - f(b_r) + f(c_r) = 2F - 2f(b_{l,r}) \geq 0.$$

  If $b_l, b_r \leq c_r < c_l$, then

  $$\Phi(c_l, b_l) - \Phi(c_r, b_r) = f(c_l) - f(b_l) - f(c_r) + f(b_r) = 0.$$

  If $b_l, b_r \geq c_l > c_r$, then

  $$\Phi(c_l, b_l) - \Phi(c_r, b_r) = f(b_l) - f(c_l) - f(b_r) + f(c_r) = 0.$$

  Finally, if $c_r \leq b_r < b_l \leq c_l$, then

  $$\Phi(c_l, b_l) - \Phi(c_r, b_r) = f(c_l) - f(b_l) - f(b_r) + f(c_r) = 2F - 2f(b_{l,r}) \geq 0.$$

- If $(c_l, c_r), (b_l, b_r) \in \mathcal{G}_2(F) \cup \mathcal{G}_3(F)$, then the pairs (b_l, b_r), (c_l, c_r) correspond to the Kruzhkov stationary solutions

  $$\tilde{b}(t, x) := b_l \mathbb{1}_{\{x<0\}} + b_r \mathbb{1}_{\{x>0\}}, \quad \tilde{c}(t, x) := c_l \mathbb{1}_{\{x<0\}} + c_r \mathbb{1}_{\{x>0\}}$$

  of the conservation law (1); inequality $\Phi(c_l, b_l) - \Phi(c_r, b_r) \geq 0$ is well known in this context (see [33]).

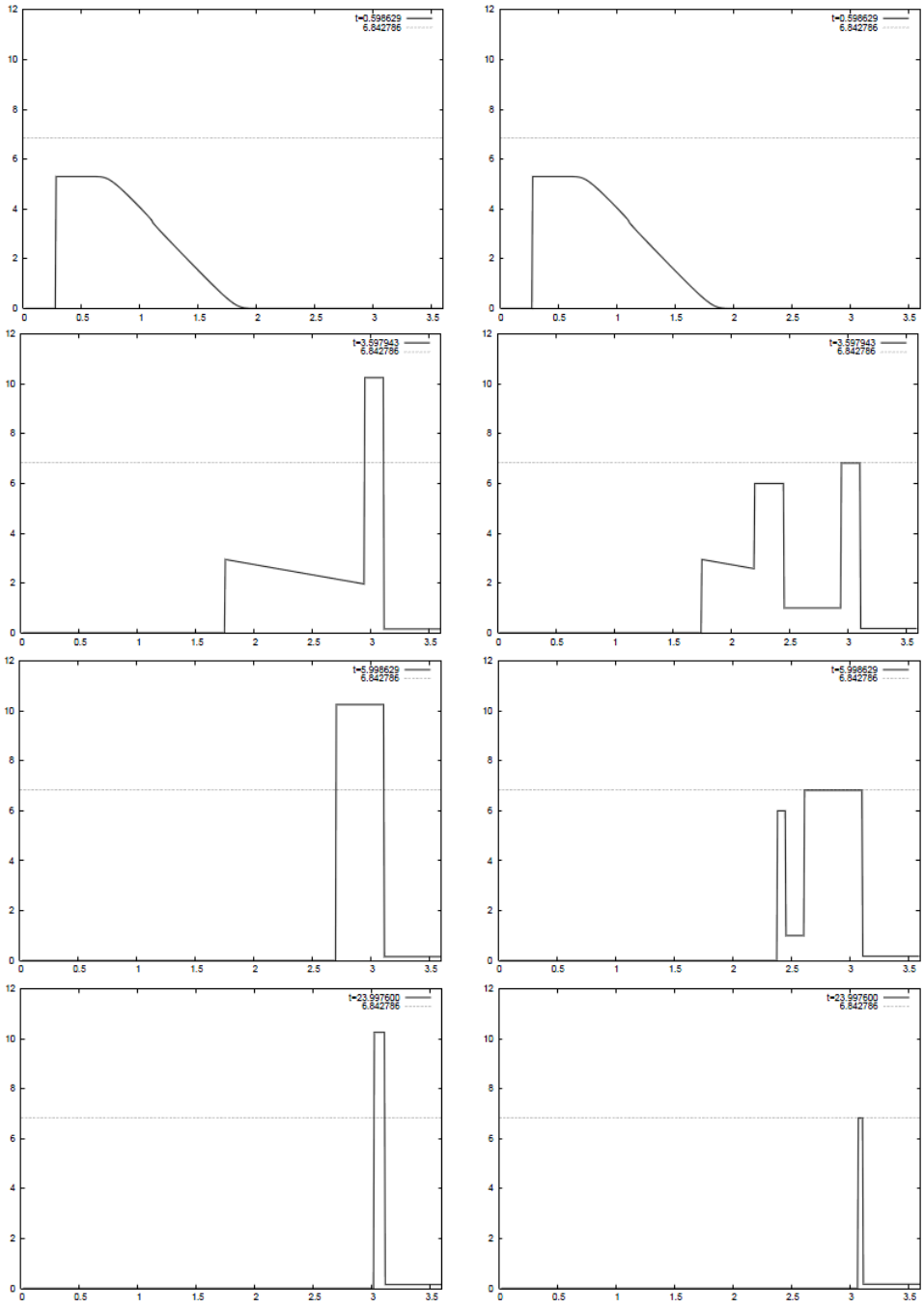

FIGURE 9. Braess paradox simulations: density profiles at times $t_1 = 0.598629$, $t_2 = 3.597943$, $t_3 = 5.998629$, $t_4 = 23.9976$, without obstacle (left) and with obstacle (right). The exit location of the exit door is $D = 3.1$ and the obstacle is located at $d = 2.45$. The horizontal dashed line represents the value of the transition between panic and non-panic densities $r = 6.842786$.

The remaining cases are deduced by symmetry of Φ; this proves (40).

(ii) Let us reason by contradiction. If $f(b_l) = f(b_r)$ but $(b_l, b_r) \notin \mathcal{G}(F)$, then either $f(b_{l,r}) > F$, or $f(b_{l,r}) < F$ and there exists $b^* \in [b_l \perp b_r, b_l \top b_r]$ such that $(b^* - b_l)(f(b^*) - f(b_l)) < 0$. In the first case, we can take $c_r < b_{l,r} < c_l$, then

$$\Phi(c_l, b_l) - \Phi(c_r, b_r) = f(c_l) - f(b_l) - f(b_r) + f(c_r) = 2F - 2f(b_{l,r}) < 0.$$

In the second case, we distinguish two subcases. If $b_r < b_l$, we can take $b_r < c_r \leq c_l < b_l$, and we get

$$\Phi(c_l, b_l) - \Phi(c_r, b_r) = f(b_l) - f(c_l) - f(c_r) + f(b_r) = 2f(b_{l,r}) - 2F < 0.$$

If $b_r > b_l$, we take $c_l = c_r = b^* \in]b_l, b_r[$ and we get

$$\Phi(b^*, b_l) - \Phi(b^*, b_r) = f(b^*) - f(b_l) - f(b_r) + f(b^*) = 2f(b^*) - 2f(b_{l,r}) < 0.$$

Thus in all the cases, we arrive to a contradiction with assumption (15).

5.2. **Proof of Theorem 2.5.** We first prove the well-posedness result in a **BV** setting. Due to the constraint (3), one cannot hope to find a uniform bound of the total variation of approximate solutions constructed by wave-front tracking (or any other approximating technique). To overcome this difficulty, we introduce an extension to the usual Temple functional [32]. We therefore define

$$\Psi(\rho) = \int_0^\rho |f'(s)| ds. \tag{41}$$

We assume that the initial datum $\rho_0 \in \mathbf{L}^\infty(\mathbb{R}; [0, R])$ satisfies $\Psi(\rho_0) \in \mathbf{BV}(\mathbb{R}; [0, R])$ and $F \in \mathbf{BV}(\mathbb{R}^+; [0, f_{\max}])$, and we follow the procedure in [12, § 4.2].

Fix a positive $n \in \mathbb{N}$, $n > 0$, and introduce in $[0, R]$ the mesh $\mathcal{M}_n$ by $\mathcal{M}_n = f^{-1}(2^{-n}\mathbb{N}) \cup \{\rho_1, \dots, \rho_N\}$. Let $\mathbf{PLC}_n$ be the set of piecewise linear and continuous functions defined on $[0, R]$ whose derivatives exist in $]0, R[\backslash \mathcal{M}_n$. Let $f^n \in \mathbf{PLC}_n$ coincide with f on $\mathcal{M}_n$.

Similarly, introduce $\mathbf{PC}_n$, respectively $\mathbf{PC}_n^+$, as the set of piecewise constant functions defined on $\mathbb{R}$, respectively $\mathbb{R}^+$, with values in $\mathcal{M}_n$, respectively in $f(\mathcal{M}_n)$. Let $F^n \in \mathbf{PC}_n^+$, coincide with F on $f(\mathcal{M}_n)$, in the sense that $F(t) = F^n(t)$ whenever $F(t) \in f(\mathcal{M}_n)$. We write

$$\begin{array}{rcll} \rho^n & = & \displaystyle\sum_\alpha \rho_\alpha^n \, \chi_{]x_{\alpha-1}, x_\alpha]} & \text{with } \rho_\alpha^n \in \mathcal{M}_n \\ F^n & = & F_0^n \, \chi_{[0,t_1]} + \displaystyle\sum_{\beta \geq 1} F_\beta^n \, \chi_{]t_\beta, t_{\beta+1}]} & \text{with } F_\beta^n \in f(\mathcal{M}_n) \end{array} \tag{42}$$

for some $x_\alpha \in \mathbb{R}$, $\alpha \in \mathbb{Z}$ (where we set $x_0 = 0$), and $t_\beta \in \mathbb{R}^+$, $\beta \in \mathbb{N}$, such that $\mathrm{TV}(F^n) \leq \mathrm{TV}(F)$. Both the approximations above are meant in the strong $\mathbf{L^1}$ topology, that is

$$\lim_{n \to +\infty} \left(\|\rho^n - \rho\|_{\mathbf{L^1}(\mathbb{R};\mathbb{R})} + \|F^n - F\|_{\mathbf{L^1}(\mathbb{R}^+;\mathbb{R})} \right) = 0 \,.$$

Let $\mathcal{D}_n = \{\rho \in \mathbf{PC}_n \colon \Psi(\rho) \in \mathbf{BV}(\mathbb{R}; \mathbb{R})\}$ and $\bar{\mathcal{D}}_n = \mathcal{D}_n \times \mathbf{PC}_n^+$. For any couple $(\rho^n, F^n) \in \bar{\mathcal{D}}_n$, written as in (42), define the Glimm type functional

$$\Upsilon(\rho^n, F^n) = \sum_\alpha \left| \Psi(\rho_{\alpha+1}^n) - \Psi(\rho_\alpha^n) \right| + 5 \sum_{t_\beta \geq 0} \left| F_{\beta+1}^n - F_\beta^n \right| + \gamma(\rho^n, F^n) \,, \tag{43}$$

where $\gamma(\rho^n, F^n)$ is defined as follows. Let $\mathcal{G}_1(F)$ be decomposed in the subsets:

$$\begin{aligned}
\mathcal{G}_1^a(F) &= \{(c_l, c_r) \in \mathcal{G}_1(F) : c_l > R_M,\ c_r < r_M\}\,,\\
\mathcal{G}_1^b(F) &= \{(c_l, c_r) \in \mathcal{G}_1(F) : c_l > R_M,\ r_M < c_r < R_M\}\,,\\
\mathcal{G}_1^c(F) &= \{(c_l, c_r) \in \mathcal{G}_1(F) : r_M < c_l < R_M,\ c_r < r_M\}\,.
\end{aligned}$$

Then, if $F^n(0) < f(r)$,

$$\gamma(\rho^n, F^n) = 0\,, \qquad \text{if } (\rho^n(0-), \rho^n(0+)) \in \mathcal{G}_1(F^n(0))\,;$$

if $F^n(0) \geq f(r)$,

$$\gamma(\rho^n, F^n) = \begin{cases} \gamma_a = 4\,(F^n(0) - f(r))\,, & \text{if } (\rho^n(0-), \rho^n(0+)) \in \mathcal{G}_1^a(F^n(0))\,,\\ \gamma_b = 4\,(f(r_M) - f(r))\,, & \text{if } (\rho^n(0-), \rho^n(0+)) \in \mathcal{G}_1^b(F^n(0))\,,\\ \gamma_c = 4\,(f(R_M) - f(r))\,, & \text{if } (\rho^n(0-), \rho^n(0+)) \in \mathcal{G}_1^c(F^n(0))\,; \end{cases}$$

otherwise

$$\gamma(\rho^n, F^n) = \gamma_o = 4\,(f(r_M) - f(r) + f(R_M) - F^n(0))\,.$$

Observe that $0 \leq \gamma(\rho^n, F^n) \leq \gamma_o$.

We then follow the nowadays classical wave-front tracking technique which dates back to [18], see also [5, § 6] and [25], or [12] for the constrained case. We fix a piecewise constant initial datum ρ_0^n such that $\mathrm{TV}(\Psi(\rho_0^n)) \leq \mathrm{TV}(\Psi(\rho_0))$ and $\lim_{n\to+\infty} \|\rho_0^n - \rho_0\|_{\mathbf{L^1}(\mathbb{R};\mathbb{R})} = 0$. At any interaction, the functional Υ either decreases by at least 2^{-n}, or remains constant with the total number of waves in the approximate solution that does not increase (see Appendix for details).

A standard application of Helly's Theorem, see [5, Theorem 2.4], yields the existence of a subsequence of approximate solutions, still denoted by ρ^n, converging in $\mathbf{L^1}_{loc}(\mathbb{R}^+ \times \mathbb{R})$ to a solution ρ of (1)-(3) in the sense of Definitions 2.2. In fact, the entropy inequality (8) is easily recovered by passing to the limit in the approximate solutions. In order to verify the constraint (9), we consider the weak formulation of (1) in the half-domain $\mathbb{R}^+ \times \mathbb{R}^+$ ($\mathbb{R}^+ \times \mathbb{R}^-$ respectively), which gives us, for all $\varphi \in \mathbf{C_c^1}(\mathbb{R}^+ \times \mathbb{R}; \mathbb{R}^+)$,

$$\begin{aligned}
\int_0^\infty \int_0^\infty (\rho^n \partial_t \varphi + f(\rho^n) \partial_x \varphi)\, dx\ dt &= \int_0^\infty \gamma_w(f(\rho^n))(t, 0+) \varphi(t, 0)\ dt\\
&= \int_0^\infty f(\rho^n(t, 0+))\ \varphi(t, 0)\ dt\\
&\leq \int_0^\infty F^n(t)\ \varphi(t, 0)\ dt
\end{aligned}$$

where $\gamma_w(f(\rho^n))(t)$ are the weak normal traces of the divergence-measure field $(\rho, f(\rho))$ defined in [10], and we have applied the Gauss-Green formula and the existence of strong traces guaranteed by [30]. Passing to the limit in the first and last integral we get

$$\begin{aligned}
\int_0^\infty F(t) \varphi(t, 0)\ dt &\geq \int_0^\infty \int_0^\infty (\rho\ \partial_t \varphi + f(\rho) \partial_x \varphi)\, dx\ dt\\
&= \int_0^\infty f(\rho(t, 0+))\ \varphi(t, 0)\ dt,
\end{aligned}$$

where the last inequality results from the fact that ρ is a weak entropy solution of (1) on $\mathbb{R}^+ \times \mathbb{R}^+$, again by [10, 30], see also [2, Remark 2]. Since the above inequality holds for all $\varphi \in \mathbf{C_c^1}(\mathbb{R}^+ \times \mathbb{R}; \mathbb{R}^+)$, we conclude that ρ satisfy (9).

To conclude the proof of Theorem 2.5, we have to verify that (17) still holds in the case of non-concave fluxes, in the **BV** setting: assume $F^1, F^2 \in \mathbf{BV}(\mathbb{R}^+; [0, f_{\max}])$, and the initial data $\rho_0^1, \rho_0^2 \in \mathbf{L}^\infty(\mathbb{R}, [0, R])$ satisfy $(\rho_0^1 - \rho_0^2) \in \mathbf{L^1}(\mathbb{R})$ and $\Psi(\rho_0^1), \Psi(\rho_0^2) \in \mathbf{BV}(\mathbb{R}; [0, R])$. We consider the entropy formulation (8) with test functions $\varphi \in \mathbf{C_c^1}(\mathbb{R}^+ \times \mathbb{R} \backslash \{x = 0\}; \mathbb{R}^+)$. The method of doubling of variables of Kruzhkov, applied in the domains $\{\pm x > 0\}$, yields the so-called Kato inequality for the comparison of ρ^1, ρ^2:

$$\int_{\mathbb{R}^+} \int_{\mathbb{R}} \Big(|\rho^1 - \rho^2| \partial_t + \Phi(\rho^1, \rho^2) \partial_x \Big) \, \varphi \, dx \, dt \geq 0.$$

Now, fix $R > 0$ and replace φ in this inequality by a sequence of approximations of the characteristic function of the set $\{t \in (0, T), 0 < |x| < R + L(T - t)\}$, for instance $\varphi_\varepsilon(t, x) = (1 - w_\varepsilon(x)) \chi_\varepsilon(t) \xi_\varepsilon(t, x)$ where

$$\chi_\varepsilon(t) = \begin{cases} 1 & \text{if } 0 \leq t < T, \\ \dfrac{T - t}{\varepsilon} + 1 & \text{if } T \leq t < T + \varepsilon, \\ 0 & \text{if } t \geq T + \varepsilon, \end{cases}$$

w_ε is given by (10), and

$$\xi_\varepsilon(t, x) = \begin{cases} 1 & \text{if } |x| \leq R + L(T - t), \\ \dfrac{R + L(T - t) - |x|}{\varepsilon} + 1 & \text{if } R + L(T - t) \leq |x| < R + L(T - t) + \varepsilon, \\ 0 & \text{if } |x| \geq R + L(T - t) + \varepsilon. \end{cases}$$

This provides at the limit $\varepsilon \to 0$

$$- \int_{-R}^{R} |\rho^1 - \rho^2|(T, x) \, dx + \int_{-R - LT}^{R + LT} |\rho_0^1 - \rho_0^2|(x) \, dx + \int_0^T \Big(\Phi(\rho^1(t, 0+), \rho^2(t, 0+)) - \Phi(\rho^1(t, 0-), \rho^2(t, 0-)) \Big) \, dt \geq 0. \quad (44)$$

Thanks to Proposition 2, we know that $(\rho^i(t, 0-), \rho^i(t, 0+)) \in \mathcal{G}(F^i)$. To conclude, we need the following Lemma.

Lemma 5.1. *For every $F^1, F^2 \in [0, f_{\max}]$ there holds*

$$\Phi(c_r^1, c_r^2) - \Phi(c_l^1, c_l^2) \leq 2 \big| F^1 - F^2 \big| \quad (45)$$

for all $(c_l^1, c_r^1) \in \mathcal{G}(F^1)$ and $(c_l^2, c_r^2) \in \mathcal{G}(F^2)$.

Proof. Without loss of generality, we can assume that $F^1 \geq F^2$. We make a case study quite similar to the one of the proof of Lemma 2.4.

- If $(c_l^i, c_r^i) \in \mathcal{G}_2(F^i) \cup \mathcal{G}_3(F^i)$, $i = 1, 2$, then both the standing waves
$$\tilde{\rho}^i(t, x) := c_l^i \mathbb{1}_{\{x < 0\}} + c_r^i \mathbb{1}_{\{x > 0\}},$$
$i = 1, 2$, are Kruzhkov entropy solutions of the (unconstrained) conservation law (1). Therefore we have the inequality
$$\Phi(c_r^1, c_r^2) - \Phi(c_l^1, c_l^2) \leq 0 \quad (46)$$
which is well known since the work of Vol′pert [33].
- If $(c_l^1, c_r^1) \in \mathcal{G}_1(F^1)$ and $(c_l^2, c_r^2) \in \mathcal{G}_2(F^2) \cup \mathcal{G}_3(F^2)$, then we can use (15) to justify (46). Indeed, the definition of $\mathcal{G}_j$ and assumption $F^1 \geq F^2$ lead to the inclusions $\mathcal{G}_j(F^2) \subset \mathcal{G}_j(F^1)$ for $j = 2, 3$.

- If $(c_l^1, c_r^1) \in \mathcal{G}_2(F^1)$ and $(c_l^2, c_r^2) \in \mathcal{G}_1(F^2)$, then $c_l^1 = c_r^1 =: c^1$, $f(c^1) \le F^1$ and $c_r^2 < c_l^2$. We have to distinguish three cases:
  - if $c^1 \le c_r^2$,
    $$\Phi(c^1, c_r^2) - \Phi(c^1, c_l^2) = f(c_r^2) - f(c^1) - f(c_l^2) + f(c^1) = 0\,;$$
  - if $c_r^2 < c^1 < c_l^2$,
    $$\Phi(c^1, c_r^2) - \Phi(c^1, c_l^2) = f(c^1) - f(c_r^2) - f(c_l^2) + f(c^1) \le 2(F^1 - F^2)\,;$$
  - if $c^1 \ge c_l^2$,
    $$\Phi(c^1, c_r^2) - \Phi(c^1, c_l^2) = f(c^1) - f(c_r^2) - f(c^1) + f(c_l^2) = 0\,.$$
- If $(c_l^1, c_r^1) \in \mathcal{G}_3(F^1)$ and $(c_l^2, c_r^2) \in \mathcal{G}_1(F^2)$, we have for sure $c_r^2 < c_l^2$. We have to detail several possibilities:
  - if $c_{l,r}^1 \le c_r^2$,
    $$\Phi(c_r^1, c_r^2) - \Phi(c_l^1, c_l^2) = f(c_r^2) - f(c_r^1) - f(c_l^2) + f(c_l^1) = 0\,;$$
  - if $c_{l,r}^1 \ge c_l^2$,
    $$\Phi(c_r^1, c_r^2) - \Phi(c_l^1, c_l^2) = f(c_r^1) - f(c_r^2) - f(c_l^1) + f(c_l^2) = 0\,;$$
  - if $c_r^2 \le c_{l,r}^1 \le c_l^2$,
    $$\Phi(c_r^1, c_r^2) - \Phi(c_l^1, c_l^2) = f(c_r^1) - f(c_r^2) - f(c_l^2) + f(c_l^1) \le 2(F^1 - F^2)\,;$$
  - if $c_r^2 \le c_l^1 \le c_l^2 \le c_r^1$,
    $$\Phi(c_r^1, c_r^2) - \Phi(c_l^1, c_l^2) = f(c_r^1) - f(c_r^2) - f(c_l^2) + f(c_l^1) \le 2(F^1 - F^2)\,;$$
  - if $c_l^1 \le c_r^2 \le c_r^1 \le c_l^2(t, 0-)$,
    $$\Phi(c_r^1, c_r^2) - \Phi(c_l^1, c_l^2) = f(c_r^1) - f(c_r^2) - f(c_l^2) + f(c_l^1) \le 2(F^1 - F^2)\,.$$
- If $(c_l^i, c_r^i) \in \mathcal{G}_1(F^i)$, $i = 1, 2$, then $f(c_{l,r}^i) = F^i$ and
  $$\Phi(c_r^1, c_r^2) - \Phi(c_l^1, c_l^2) \le \left|f(c_r^1) - f(c_r^2)\right| + \left|f(c_l^1) - f(c_l^2)\right| = 2(F^1 - F^2).$$

Thus in all cases, we have

$$\Phi(c_r^1, c_r^2) - \Phi(c_l^1, c_l^2) \le 2|F^1 - F^2|(t).$$

□

From (44) and (45) we have

$$\int_{-R}^{R} |\rho^1 - \rho^2|(T, x)\, dx \le \int_0^T 2|F^1 - F^2|(t)\, dt + \int_{-R-LT}^{R+LT} |\rho_0^1 - \rho_0^2|(x)\, dx;$$

letting R tend to $+\infty$, we recover (17) for data of the **BV** setting.

Let us turn now on the $\mathbf{L}^\infty$ setting. One may remark that the proof of (17) is also valid for data ρ_0 and F in $\mathbf{L}^\infty$. In order to obtain the existence result in the general $\mathbf{L}^\infty$ case, we have to construct, from an initial datum $\rho_0 \in \mathbf{L}^\infty(\mathbb{R})$ and a constraint $F \in \mathbf{L}^\infty(\mathbb{R}^+)$, a sequence of initial data $(\rho_0^n)_{n\ge0}$ and a sequence of constraints $(F^n)_{n\ge0}$ which satisfy the aforementioned **BV** assumptions, using classical trunctation functions and mollifiers, such that

$$\rho_0^n \to \rho_0 \text{ in } \mathbf{L^1}_{loc}(\mathbb{R}) \text{ and a.e.;} \quad F^n \to F \text{ in } \mathbf{L^1}_{loc}(\mathbb{R}^+) \text{ and a.e. .}$$

Following [2], if $(\rho^n)_{n\ge0}$ denotes the sequence of associated weak entropy solutions (in the sense of Definition 2.2 or Definition 2.3), one could try to pass to the limit in the last integral of (14) to obtain a solution ρ in $\mathbf{L}^\infty(\mathbb{R}^+ \times \mathbb{R})$. But in the present

(non-concave) case the map $F \mapsto \mathrm{dist}\,((c_l, c_r), \mathcal{G}(F))$ is not continuous as a map in $\mathbf{L^1}_{loc}(\mathbb{R}^+)$ with values in $\mathbb{R}^+$. We use instead Definition 2.2: the convergence in (8) is classical while the constraint (9) becomes when $n \to +\infty$

$$\gamma^-[f(\rho)](t) = \gamma^+[f(\rho)](t) \leq F(t)$$

where $\gamma^\pm$ are the left and right trace operators. The convergence of the traces of the flux is possible using the compactness result for conservation laws in bounded domains stated for instance in [29, Remark 7.33, Chapter 2].

Appendix.

Lemma 5.2. *For any $n \in \mathbb{N}$ and $(\rho_o^n, F^n) \in \bar{\mathcal{D}}_n$, let ρ^n be the approximate solution to (1)-(3) obtained by wave-front tracking. At any waves interaction, the map $t \mapsto \Upsilon(t) = \Upsilon\left(\rho^n(t), F^n(\cdot + t)\right)$*

either: *decreases by at least 2^{-n},*

or: *remains constant and the number of waves does not increase.*

Proof. The proof is obtained considering the different interactions separately, depending on the position of the interaction point $\bar{x}$ and on the flows of the interacting states. We will consider interaction points $\bar{x} \leq 0$, the case $\bar{x} \geq 0$ being symmetric. It is not restrictive to assume that at any interaction time either two waves interact or a single wave hits $x = 0$.

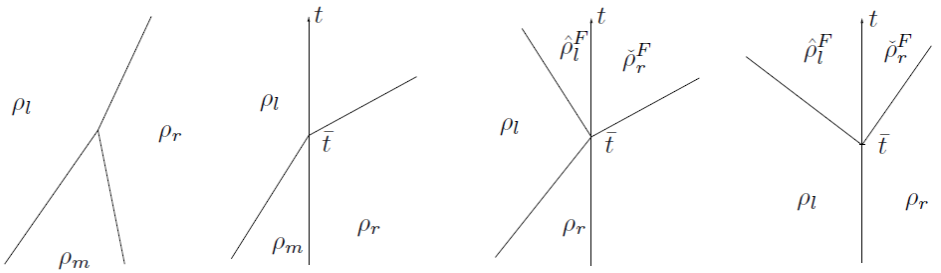

FIGURE 10. Notations for the proof of Lemma 5.2.

(I1) $\bar{x} \neq 0$. As in the classical scalar case, either the two jumps have the same sign, and the interaction results in a single discontinuity (and the number of waves diminishes), or the jumps have opposite sign, and $\mathrm{TV}(\Psi(\rho))$ decreases by at least 2^{-n+1}, seealso [5, § 6.1], see Figure 10, left.

(I2) A wave hits $\bar{x} = 0$ at time $t = \bar{t}$ coming from the left. We have to distinguish between several situations.
Assume first that $\rho_m = \rho_r$. If $\mathcal{R}^F(\rho_l, \rho_r) = \mathcal{R}(\rho_l, \rho_r)$, then the wave simply crosses $x = 0$ and $\Delta\Upsilon(\bar{t}) = \Upsilon(\bar{t}+) - \Upsilon(\bar{t}-) = 0$. Otherwise, $f(\rho_l) > F$ and $\hat{\rho}_l^F > \rho_l$. This implies

$$\begin{aligned}\Delta\Upsilon(\bar{t}) &= \left|\Psi(\rho_l) - \Psi(\hat{\rho}_l^F)\right| + \left|\Psi(\hat{\rho}_l^F) - \Psi(\check{\rho}_r^F)\right| \\ &\quad + \left|\Psi(\check{\rho}_l^F) - \Psi(\rho_r)\right| + \gamma - \left|\Psi(\rho_l) - \Psi(\rho_r)\right| - \gamma_o \\ &= 2\Psi(\hat{\rho}_l^F) - 2\Psi(\rho_l) + \gamma - \gamma_o \leq -2^{1-n}.\end{aligned}$$

Above, $\gamma = 0, \gamma_a, \gamma_b, \gamma_c$ depending on the situation.

Let us consider now the case in which the wave (ρ_m, ρ_r) is an entropic shock or a rarefaction wave satisfying the constraint. If $\mathcal{R}^F(\rho_l, \rho_r) = \mathcal{R}(\rho_l, \rho_r)$, we

are exactly in the case (I1).
If $\mathcal{R}^F(\rho_l,\rho_r)\neq\mathcal{R}(\rho_l,\rho_r)$, we have $\rho_l>\rho_r$ and $f(\rho_m)=f(\rho_r)\leq F$, hence $\check\rho_r^F\geq\rho_r$. We can estimate

$$\begin{aligned}\Delta\Upsilon(\bar t) &\leq \left|\Psi(\rho_l)-\Psi(\hat\rho_l^F)\right|+\left|\Psi(\hat\rho_l^F)-\Psi(\check\rho_r^F)\right|\\ &\quad+\left|\Psi(\check\rho_r^F)-\Psi(\rho_r)\right|+\gamma-\left|\Psi(\rho_l)-\Psi(\rho_r)\right|-\gamma_o.\end{aligned}$$

If $\rho_l\geq\hat\rho_l^F$, we have $\Delta\Upsilon(\bar t)\leq\gamma-\gamma_0\leq-2^{2-n}$. If $\rho_l<\hat\rho_l^F$ (and hence $f(\rho_l)>F$), we obtain

$$\Delta\Upsilon(\bar t)\leq 2\Psi(\hat\rho_l^F)-2\Psi(\rho_l)+\gamma-\gamma_o\leq-2^{1-n}.$$

Assume now that the wave $(\rho_m,\rho_r)\in\mathcal{G}_1$ is a non-classical shock resulting from the application of $\mathcal{R}^F$. If the segment joining $f(\rho_m)$ and $f(\rho_r)$ does not intersect the graph of f, then $\rho_l<\rho_r$, no new wave is created and easy calculations show that

$$\begin{aligned}\Delta\Upsilon(\bar t) &= |\Psi(\rho_l)-\Psi(\rho_r)|+\gamma_o\\ &\quad-|\Psi(\rho_l)-\Psi(\rho_m)|-|\Psi(\rho_m)-\Psi(\rho_r)|\\ &= 2\Psi(\rho_r)-2\Psi(\rho_m)+\gamma_o=0.\end{aligned}$$

If $(\rho_m,\rho_r)\in\mathcal{G}_1^a$ and $F^n(\bar t)>f(r)$, then $\rho_l\geq r$ and we have

$$\begin{aligned}\Delta\Upsilon(\bar t) &= \left|\Psi(\rho_l)-\Psi(\hat\rho_l^F)\right|+\left|\Psi(\hat\rho_l^F)-\Psi(\rho_r)\right|+\gamma_c\\ &\quad-|\Psi(\rho_l)-\Psi(\rho_m)|-|\Psi(\rho_m)-\Psi(\rho_r)|-\gamma_a\\ &= 2\Psi(\rho_l)-2\Psi(\rho_m)+\gamma_c-\gamma_a\\ &= 2(f(\rho_l)-F^n(\bar t))\leq-2^{1-n}.\end{aligned}$$

The case $(\rho_m,\rho_r)\in\mathcal{G}_1^b$ is similar. Finally, if $(\rho_m,\rho_r)\in\mathcal{G}_1^c$, we have to distinguish two cases, depending on the position of ρ_l. If $\rho_l<\rho_r$, the case can be treated as above. If $r<\rho_l<R_M$, then $\hat\rho_l^F>\rho_l$ and $(\hat\rho_l^F,\rho_r)\in\mathcal{G}_1^a$. Then the number of waves remains constant and

$$\begin{aligned}\Delta\Upsilon(\bar t) &= \left|\Psi(\rho_l)-\Psi(\hat\rho_l^F)\right|+\left|\Psi(\hat\rho_l^F)-\Psi(\rho_r)\right|+\gamma_a\\ &\quad-|\Psi(\rho_l)-\Psi(\rho_m)|-|\Psi(\rho_m)-\Psi(\rho_r)|-\gamma_c\\ &= 2\Psi(\hat\rho_l^F)-2\Psi(\rho_l)+\gamma_a-\gamma_c\leq 0.\end{aligned}$$

(I3) A wave hits $\bar x=0$ at time $t=\bar t$ coming from the right. If $\rho_l=\rho_m$ and $\mathcal{R}^F(\rho_l,\rho_r)\neq\mathcal{R}(\rho_l,\rho_r)$, then it must be $f(\rho_r)>F$ and $\check\rho_r^F<\rho_r$ (and $f(\rho_l)\leq F$ and $\hat\rho_l^F\leq\rho_l$). We have

$$\begin{aligned}\Delta\Upsilon(\bar t) &= \left|\Psi(\rho_l)-\Psi(\hat\rho_l^F)\right|+\left|\Psi(\hat\rho_l^F)-\Psi(\check\rho_r^F)\right|\\ &\quad+\left|\Psi(\check\rho_l^F)-\Psi(\rho_r)\right|+\gamma-\left|\Psi(\rho_l)-\Psi(\rho_r)\right|-\gamma_o\\ &= 2\Psi(\rho_r)-2\Psi(\check\rho_r^F)+\gamma-\gamma_o\\ &\leq 2\left(F-f(\rho_r)\right)\leq-2^{1-n}.\end{aligned}$$

Above, $\gamma=0,\gamma_a,\gamma_b,\gamma_c$ depending on the situation.

Let us now assume that (ρ_l,ρ_m) is an entropic shock or rarefaction wave, and $\mathcal{R}^F(\rho_l,\rho_r)\neq\mathcal{R}(\rho_l,\rho_r)$. Then we have $f(\rho_l)=f(\rho_m)\leq F$, and thus

$\hat\rho_l^F \le \rho_l$. Moreover, $\rho_r < \rho_l$. Then

$$\begin{aligned}\Delta\Upsilon(\bar t) &\le \left|\Psi(\rho_l)-\Psi(\hat\rho_l^F)\right| + \left|\Psi(\hat\rho_l^F)-\Psi(\check\rho_r^F)\right| \\ &\quad + \left|\Psi(\check\rho_r^F)-\Psi(\rho_r)\right| + \gamma - \left|\Psi(\rho_l)-\Psi(\rho_r)\right| - \gamma_o \\ &= \Psi(\rho_r)-\Psi(\check\rho_r^F) + \left|\Psi(\check\rho_r^F)-\Psi(\rho_r)\right| + \gamma - \gamma_o.\end{aligned}$$

If $\rho_r \le \check\rho_r^F$, we have $\Delta\Upsilon(\bar t) \le \gamma - \gamma_0 \le -2^{2-n}$. If $\rho_l > \hat\rho_l^F$ (and hence $f(\rho_r) > F$), we obtain

$$\Delta\Upsilon(\bar t) \le 2\Psi(\rho_r) - 2\Psi(\check\rho_r^F) + \gamma - \gamma_o \le 2\left(F - f(\rho_r)\right) \le -2^{1-n}.$$

Assume now that the wave $(\rho_l,\rho_m) \in \mathcal{G}_1$ is a non-classical shock resulting from the application of $\mathcal{R}^F$. If the segment joining $f(\rho_l)$ and $f(\rho_m)$ does not intersect the graph of f, then $\rho_l < \rho_r$, no new wave is created and easy calculations show that

$$\begin{aligned}\Delta\Upsilon(\bar t) &= \left|\Psi(\rho_l)-\Psi(\rho_r)\right| + \gamma_o \\ &\quad - \left|\Psi(\rho_l)-\Psi(\rho_m)\right| - \left|\Psi(\rho_m)-\Psi(\rho_r)\right| \\ &= 2\Psi(\rho_m) - 2\Psi(\rho_l) + \gamma_o = 0.\end{aligned}$$

If $(\rho_l,\rho_m) \in \mathcal{G}_1^a$ and $F^n(\bar t) > f(r)$, then the case $\rho_l < \rho_r$ can be treated as the previous case. Otherwise, if $r_M < \rho_r \le r$, we have

$$\begin{aligned}\Delta\Upsilon(\bar t) &= \left|\Psi(\rho_l)-\Psi(\check\rho_r^F)\right| + \left|\Psi(\check\rho_r^F)-\Psi(\rho_r)\right| + \gamma_b \\ &\quad - \left|\Psi(\rho_l)-\Psi(\rho_m)\right| - \left|\Psi(\rho_m)-\Psi(\rho_r)\right| - \gamma_a \\ &= 2\Psi(\rho_m) - 2\Psi(\rho_r) + \gamma_b - \gamma_a \\ &= 2(f(\rho_r) - F^n) \le -2^{1-n}.\end{aligned}$$

The case $(\rho_l,\rho_m) \in \mathcal{G}_1^c$ is similar. Finally, if $(\rho_l,\rho_m) \in \mathcal{G}_1^b$, we have to distinguish two cases, depending on the position of ρ_r. If $\rho_r > \rho_m$, the case can be treated as above. If $\rho_r < \rho_m \le r$, then $f(\rho_r) > F$ and $\check\rho_r^F < \rho_r$ and $(\rho_l,\check\rho_r^F) \in \mathcal{G}_1^a$. Then the number of waves remains constant and

$$\begin{aligned}\Delta\Upsilon(\bar t) &= \left|\Psi(\rho_l)-\Psi(\check\rho_r^F)\right| + \left|\Psi(\check\rho_r^F)-\Psi(\rho_r)\right| + \gamma_a \\ &\quad - \left|\Psi(\rho_l)-\Psi(\rho_m)\right| - \left|\Psi(\rho_m)-\Psi(\rho_r)\right| - \gamma_b \\ &= 2\Psi(\rho_r) - 2\Psi(\check\rho_r^F) + \gamma_a - \gamma_b \\ &= 2\left(F - f(\rho_r)\right) \le 0.\end{aligned}$$

(I4) The constraint F^n jumps downward, see Fig. 10, right. We have to check several cases.
If $\rho_l = \rho_r = \rho$ and $F^n(\bar t+) < f(\rho) \le F^n(\bar t-)$, two waves will exit the point $(\bar t, 0)$ with $\check\rho^F < \rho < \hat\rho^F$:

$$\begin{aligned}\Delta\Upsilon(\bar t) &= \left|\Psi(\rho)-\Psi(\hat\rho^F)\right| + \left|\Psi(\hat\rho^F)-\Psi(\check\rho^F)\right| \\ &\quad + \left|\Psi(\check\rho^F)-\Psi(\rho)\right| + \gamma - \gamma_o - 5\left|F^n(\bar t+) - F^n(\bar t-)\right| \\ &= 2\Psi(\hat\rho^F) - 2\Psi(\check\rho^F) + \gamma - \gamma_o - 5\left|F^n(\bar t+) - F^n(\bar t-)\right| \\ &= -5\left|F^n(\bar t+) - F^n(\bar t-)\right| \le -5\times 2^{-n}.\end{aligned}$$

Above, $\gamma = 0, \gamma_b$ or γ_c, depending on the position of ρ.
If (ρ_l,ρ_r) is an entropic shock, and $F^n(\bar t+) < f(\rho_l) = f(\rho_r) \le F^n(\bar t-)$, then

$$\begin{aligned}\Delta\Upsilon(\bar t) &= \left|\Psi(\rho_l)-\Psi(\hat\rho_l^F)\right| + \left|\Psi(\hat\rho_l^F)-\Psi(\check\rho_r^F)\right| + \left|\Psi(\check\rho_r^F)-\Psi(\rho_r)\right| \\ &\quad + \gamma - \left|\Psi(\rho_l)-\Psi(\rho_r)\right| - \gamma_o - 5\left|F^n(\bar t+) - F^n(\bar t-)\right|.\end{aligned}$$

Therefore, if $\rho_r < r < \rho_l$, then $\check{\rho}_r^F < \rho_r < \rho_l < \hat{\rho}_l^F$ and $(\hat{\rho}_l^F, \check{\rho}_r^F) \in \mathcal{G}_1^a$:

$$\begin{aligned}\Delta\Upsilon(\bar{t}) &\leq 2\Psi(\hat{\rho}_l^F) - 2\Psi(\check{\rho}_r^F) + 2\Psi(\rho_r) - 2\Psi(\rho_l)\\ &\quad +\gamma_a - \gamma_o - 5\left(F^n(\bar{t}-) - F^n(\bar{t}+)\right)\\ &= -4\left(f(\rho_l) - f(r)\right) + 4\left(F^n(\bar{t}+) - f(r)\right) - \left(F^n(\bar{t}-) - F^n(\bar{t}+)\right)\\ &\leq -2^{-n};\end{aligned}$$

otherwise, if $\rho_l < \rho_r$, then $\check{\rho}_r^F < \rho_l < \rho_r < \hat{\rho}_l^F$:

$$\begin{aligned}\Delta\Upsilon(\bar{t}) &\leq 2\Psi(\hat{\rho}_l^F) - 2\Psi(\check{\rho}_r^F) + \gamma - \gamma_o - 5\left(F^n(\bar{t}-) - F^n(\bar{t}+)\right)\\ &= -\left(F^n(\bar{t}-) - F^n(\bar{t}+)\right) \leq -2^{-n}.\end{aligned}$$

Finally, if (ρ_l, ρ_r) is a non-classical shock, and $F^n(\bar{t}+) < f(\rho_l) = f(\rho_r) = F^n(\bar{t}-)$, then $\check{\rho}_r^F < \rho_r < \rho_l < \hat{\rho}_l^F$ and

$$\begin{aligned}\Delta\Upsilon(\bar{t}) &\leq 2\Psi(\hat{\rho}_l^F) - 2\Psi(\check{\rho}_r^F) + 2\Psi(\rho_r) - 2\Psi(\rho_l)\\ &\quad +\gamma(\bar{t}+) - \gamma(\bar{t}-) - 5\left(F^n(\bar{t}-) - F^n(\bar{t}+)\right)\\ &\leq -\left(F^n(\bar{t}-) - F^n(\bar{t}+)\right) \leq -2^{-n}.\end{aligned}$$

(I5) The constraint F^n jumps upward. We need to check only the case in which (ρ_l, ρ_r) is a non-classical shock, and $F^n(\bar{t}+) > f(\rho_l) = f(\rho_r) = F^n(\bar{t}-)$. If $f\left(\mathcal{R}(\rho_l, \rho_r)(0)\right) \leq F^n(\bar{t}+)$, then the solution becomes classical and the variation of the functional can be estimated as follows

$$\begin{aligned}\Delta\Upsilon(\bar{t}) &= |\Psi(\rho_l) - \Psi(\rho_r)| + \gamma_o(\bar{t}+)\\ &\quad -|\Psi(\rho_l) - \Psi(\rho_r)| - \gamma(\bar{t}-) - 5\left(F^n(\bar{t}-) - F^n(\bar{t}+)\right)\\ &\leq -\left(F^n(\bar{t}-) - F^n(\bar{t}+)\right) \leq -2^{-n}.\end{aligned}$$

Otherwise, if $f\left(\mathcal{R}(\rho_l, \rho_r)(0)\right) > F^n(\bar{t}+)$, we still have a nonclassical shock and $\rho_r < \check{\rho}_r^F < \hat{\rho}_l^F < \rho_l$:

$$\begin{aligned}\Delta\Upsilon(\bar{t}) &= \left|\Psi(\hat{\rho}_l^F) - \Psi(\check{\rho}_r^F)\right| + \gamma(\bar{t}+)\\ &\quad -|\Psi(\rho_l) - \Psi(\rho_r)| - \gamma(\bar{t}-) - 5\left(F^n(\bar{t}-) - F^n(\bar{t}+)\right)\\ &\leq -\left(F^n(\bar{t}-) - F^n(\bar{t}+)\right) \leq -2^{-n}.\end{aligned}$$

Indeed, observe that

$$\left|\Psi(\hat{\rho}_l^F) - \Psi(\check{\rho}_r^F)\right| \leq |\Psi(\rho_l) - \Psi(\rho_r)|$$

and

$$\gamma(\bar{t}+) - \gamma(\bar{t}-) - 5\left(F^n(\bar{t}-) - F^n(\bar{t}+)\right) \leq -\left(F^n(\bar{t}-) - F^n(\bar{t}+)\right).$$

□

Acknowledgments. The authors would like to thank the anonymous referees for their valuable comments that allowed to improve the paper.

REFERENCES

[1] B. Andreianov and N. Seguin, *Analysis of a Burgers equation with singular resonant source term and convergence of well-balanced schemes*, Discrete Contin. Dyn. Syst., **32** (2012), 1939–1964.

[2] B. Andreianov, P. Goatin and N. Seguin, *Finite volume schemes for locally constrained conservation laws*, With supplementary material available online, Numer. Math., **115** (2010), 609–645.

[3] B. Andreianov, K. H. Karlsen and N. H. Risebro, *A theory of L^1-dissipative solvers for scalar conservation laws with discontinuous flux*, Arch. Ration. Mech. Anal., **201** (2011), 27–86.

[4] D. Braess, *Über ein Paradoxon aus der Verkehrsplanung*, Unternehmensforschung, **12** (1968), 258–268.
[5] A. Bressan, "Hyperbolic Systems of Conservation Laws. The One-Dimensional Cauchy Problem," Oxford Lecture Series in Mathematics and its Applications, Vol. 20, Oxford University Press, Oxford, 2000.
[6] R. Bürger, A. García, K. H. Karlsen and J. D. Towers, *A family of numerical schemes for kinematic flows with discontinuous flux*, J. Engrg. Math., **60** (2008), 387–425.
[7] C. Cancès and N. Seguin, *Error estimate for Godunov approximation of locally constrained conservation laws*, SIAM J. Numer. Anal., **50** (2012), 3036–3060.
[8] C. Chalons, *Numerical approximation of a macroscopic model of pedestrian flows*, SIAM J. Sci. Comput., **29** (2007), 539–555 (electronic).
[9] C. Chalons and P. Goatin, *Godunov scheme and sampling technique for computing phase transitions in traffic flow modeling*, Interfaces Free Bound., **10** (2008), 197–221.
[10] G.-Q. Chen and H. Frid, *Divergence-measure fields and hyperbolic conservation laws*, Arch. Ration. Mech. Anal., **147** (1999), 89–118.
[11] P. Colella, *Glimm's method for gas dynamics*, SIAM J. Sci. Statist. Comput., **3** (1982), 76–110.
[12] R. M. Colombo and P. Goatin, *A well posed conservation law with a variable unilateral constraint*, J. Differential Equations, **234** (2007), 654–675.
[13] R. M. Colombo, P. Goatin and M. D. Rosini, *Conservation laws with unilateral constraints in traffic modeling*, Applied and Industrial Mathematics in Italy III, Ser. Adv. Math. Appl. Sci., **82**, World Sci. Publ., Hackensack, NJ, (2010), 244–255.
[14] ———, *On the modelling and management of traffic*, ESAIM Math. Model. Numer. Anal., **45** (2011), 853–872.
[15] R. M. Colombo and M. D. Rosini, *Pedestrian flows and non-classical shocks*, Math. Methods Appl. Sci., **28** (2005), 1553–1567.
[16] ———, *Existence of nonclassical solutions in a pedestrian flow model*, Nonl. Analysis: RWA, **10** (2009), 2716–2728.
[17] M. G. Crandall and L. Tartar, *Some relations between nonexpansive and order preserving mappings*, Proc. AMS, **78** (1980), 385–390.
[18] C. M. Dafermos, *Polygonal approximations of solutions of the initial value problem for a conservation law*, J. Math. Anal. Appl., **38** (1972), 33–41.
[19] M. L. Delle Monache and P. Goatin, *Scalar conservation laws with moving density constraints arising in traffic flow modeling*, INRIA Research Report, no. 8119, October 2012.
[20] R. Eymard, T. Gallouët and R. Herbin, *Finite volume methods*, in "Handbook of Numerical Analysis," Vol. VII, Handb. Numer. Anal., **VII**, North-Holland, Amsterdam, (2000), 713–1020.
[21] M. Garavello and P. Goatin, *The Aw-Rascle traffic model with locally constrained flow*, J. Math. Anal. Appl., **378** (2011), 634–648.
[22] M. Garavello and B. Piccoli, "Traffic Flow on Networks. Conservation Laws Models," AIMS Series on Applied Mathematics, **1**, American Institute of Mathematical Sciences (AIMS), Springfield, MO, 2006.
[23] I. M. Gel′fand, *Some problems in the theory of quasi-linear equations*, Uspehi Mat. Nauk, **14** (1959), 87–158.
[24] D. Helbing, A. Johansson, and H. Z. Al-Abideen, *Dynamics of crowd disasters: An empirical study*, Physical Review E, **75** (2007).
[25] H. Holden and N. H. Risebro, "Front Tracking for Hyperbolic Conservation Laws," Applied Mathematical Sciences, Vol. 152, Springer-Verlag, New York, 2002.
[26] S. N. Kružhkov, *First order quasilinear equations with several independent variables*, Mat. Sb. (N.S.), **81** (1970), 228–255.
[27] P. G. LeFloch, "Hyperbolic Systems of Conservation Laws. The Theory of Classical and Nonclassical Shock Waves," Lectures in Mathematics ETH Zürich, Birkhäuser Verlag, Basel, 2002.
[28] T. P. Liu, *The Riemann problem for general systems of conservation laws*, J. Differential Equations, **18** (1975), 218–234.
[29] J. Málek, J. Nečas, M. Rokyta and M. Růžička, "Weak and Measure-Valued Solutions to Evolutionary PDEs," Applied Mathematics and Mathematical Computation, **13**, Chapman & Hall, London, 1996.

[30] E. Yu. Panov, *Existence of strong traces for quasi-solutions of multidimensional conservation laws*, J. Hyperbolic Differ. Equ., **4** (2007), 729–770.
[31] M. D. Rosini, *Nonclassical interactions portrait in a macroscopic pedestrian flow model*, J. Differential Equations, **246** (2009), 408–427.
[32] B. Temple, *Global solution of the Cauchy problem for a class of* 2×2 *nonstrictly hyperbolic conservation laws*, Adv. in Appl. Math., **3** (1982), 335–375.
[33] A. I. Vol′pert, *Spaces* BV *and quasilinear equations*, Mat. Sb. (N.S.), **73(115)** (1967), 255–302.

Received July 2012; revised November 2012.

E-mail address: christophe_chalons@ljll.univ-paris-diderot.fr
E-mail address: paola.goatin@inria.fr
E-mail address: nicolas.seguin@upmc.fr